


# INVESTIGATION OF DECARBONISATION PATHWAYS FOR SHORT HAUL AVIATION USING A DISCRETE OPTIMISATION DECISION-MAKING ALGORITHM

Naoise Barry[1], Conor Gallagher[1] and Charles Stuart[1]

[1]Trinity College Dublin, The University of Dublin, Ireland.

## Abstract

This work utilises a decarbonisation evaluation framework for sustainable aviation concepts to analyse the impact alternative energy carriers may have. Three alternative energy carriers are studied, namely liquid natural gas (LNG), renewable natural gas (RNG) and liquid hydrogen ($LH_2$). These alternative energy carriers necessitate aircraft design re-configurations which are modelled within the aircraft performance sub-model of this framework. These fuel-specific re-configurations of the base aircraft design have associated changes to the fuel consumption and emissions production characteristics which are evaluated and stored in a digital hangar database from which the scheduling sub-model component of the framework can objectively assess the optimal allocation of flights to these alternative aircraft variants. Through this framework, the decarbonisation potential of the alternative energy carriers may be assessed within operational scenarios for various levels of emissions reduction potential, fuel pricing, fleet composition and emissions' penalisation. The evaluation is based on a holistic sustainability score which is measured as the simultaneous maintenance or improvement of the economic viability while minimising the environmental impact of the given decarbonisation concept. This holistic nature for operational scenarios enables objective comparisons to be drawn between the alternative energy carrier scenarios and a 2035 baseline fleet of conventional B737-8200 MAX aircraft fuelled by a sustainable aviation fuel blend. Through these comparative studies, it was found that natural gas in both forms, fossil LNG and the lower carbon-intensity RNG, offer holistic sustainability gains relative to the baseline. While the RNG scenarios offered the greatest improvement in sustainability performance, this came with the drawback of a significant increase in energy demand due to the high generation energy required for RNG. The LNG scenarios still offered sustainability improvements but with a much lesser energy demand, therefore indicating that natural gas, whether it be from fossil or renewable sources, still offers considerable holistic sustainability benefits and promote its inclusion as a decarbonisation pathway for the sector. The $LH_2$ scenarios suffered from relatively higher in-flight energy penalties and were only operable in the best-case operational scenarios for costs, thus drawing attention to the imperative need for the design of decarbonisation concepts to be cognisant of and interlinked to the application phase to leverage potential decarbonisation benefits.

**Keywords:** Decarbonisation, alternative energy carriers, operations, decision-making, discrete optimisation

## Nomenclature

**Greek Symbols**

| | | |
|---|---|---|
| $\alpha_p$ | = | Passenger revenue (€) |
| $\beta_C$ | = | Crew costs (€) |
| $\beta_E$ | = | Emissions' costs (€) |
| $\beta_F$ | = | Fuel costs (€) |
| $\beta_H$ | = | Handling costs (€) |
| $\beta_L$ | = | Landing costs (€) |
| $\gamma$ | = | Objective score (€) |
| $\eta_p$ | = | Production efficiency (%) |
| $\theta$ | = | Flight path angle (rad) |
| $\mu_{LHV}$ | = | Ratio of lower-heating values (-) |
| $\rho$ | = | Air density (kg/m$^3$) |
| $\phi_C$ | = | Crew costs matrix (€) |
| $\phi_E$ | = | Emissions' costs matrix (€) |
| $\phi_F$ | = | Fuel costs matrix (€) |
| $\phi_H$ | = | Handling costs matrix (€) |
| $\phi_L$ | = | Landing costs matrix (€) |
| $\phi_{p,b}$ | = | Base passenger revenue matrix (€) |
| $\phi_{p,d}$ | = | Distance passenger revenue matrix (€) |

**Letters**

| | | | | | |
|---|---|---|---|---|---|
| $C_D$ | = | Drag coefficient (-) | $L$ | = | Lift (N) |
| $C_{D,0}$ | = | Zero-lift drag coefficient (-) | $Ma$ | = | Mach number (-) |
| $C_L$ | = | Lift coefficient (-) | $\dot{m}_f$ | = | Fuel consumption rate (kg/s) |
| $D$ | = | Drag (N) | $m_f$ | = | Fuel consumption (kg) |
| $d_m$ | = | Mission range (m) | $\overline{m}_p$ | = | Average passenger mass (kg) |
| $E_{cons}$ | = | Consumed energy (J) | $n_p$ | = | Number of passengers (-) |
| $e_f$ | = | $CO_2$ emissions (kg) | $p$ | = | Fuel price (€/L) |
| $E_{fuel}$ | = | Consumable fuel energy (J) | $S$ | = | Area ($m^2$) |
| $E_{gen}$ | = | Generation energy requirement (J) | $t$ | = | Segment timestep (s) |
| $E_{RPK}$ | = | Revenue passenger energy (J) | $T$ | = | Thrust (N) |
| $f_L$ | = | Landing fuel (L) | $V_\infty$ | = | True airspeed (m/s) |
| $f_M$ | = | Mission fuel (L) | $V_H$ | = | Vertical velocity (m/s) |
| $f_R$ | = | Reserve mission fuel (L) | $V_V$ | = | Horizontal velocity (m/s) |
| $f_{TO}$ | = | Take-off fuel (L) | $W$ | = | Weight (N) |
| $g$ | = | Acceleration due to gravity ($m/s^2$) | $x$ | = | Horizontal displacement (m) |
| $k$ | = | Induced drag factor (-) | $y$ | = | Vertical displacement (m) |

**Acronyms**

| | | | | | |
|---|---|---|---|---|---|
| ASK | = | Available seat kilometres (km) | MTOW | = | Maximum take-off weight (kg) |
| ASTM | = | American Society for Testing and Materials | NG | = | Natural gas |
| ATAG | = | Air Transport Action Group | OEW | = | Operating empty weight (kg) |
| CI | = | Carbon-intensity ($gCO_2/MJ$) | PSEC | = | Productivity specific energy consumption (-) |
| $CO_2$ | = | Carbon dioxide | PtL | = | Power-to-Liquid |
| ETS | = | Emission's trading system | RNG | = | Renewable natural gas |
| EU | = | European Union | RPK | = | Revenue passenger kilometres (km) |
| FLEET | = | Fleet-Level Environmental Evaluation Tool | RTB | = | Return to base |
| FT | = | Fischer-Tropsch | SAF | = | Sustainable aviation fuel |
| GDP | = | Gross domestic product ($ or €) | SUAVE | = | Stanford University aerospace vehicle environment |
| GHG | = | Greenhouse gas | TAS | = | True airspeed (m/s) |
| GI | = | Gravimetric index (%) | TLAR | = | Top level aircraft requirements |
| HEFA | = | Hydroprocessed Esters and Fatty Acids | TOW | = | Take-off weight (kg) |
| IATA | = | International Air Transport Association | TRL | = | Technology readiness level |
| ICAO | = | International Civil Aviation Organisation | TSFC | = | Thrust specific fuel consumption (kg/s.kN) |
| $LH_2$ | = | Liquid hydrogen | TtW | = | Tank-to-Wake |
| LHV | = | Lower-heating value (MJ/kg) | UN | = | United Nations |
| LNG | = | Liquid natural gas | UNFCCC | = | United Nations' Framework Convention on Climate Change |
| LTAG | = | Long-Term Aspirational Goals | WtT | = | Well-to-Tank |
| MILP | = | Mixed-integer linear programming | WtW | = | Well-to-Wake |

## 1. Introduction

Civil aviation is a key contributor to the global gross domestic product (GDP) at $3.5 trillion in 2024 [1] with the aviation related GDP in Europe being more than €760 billion [2]. In 2023, the aviation sector was responsible for 2.05% of global $CO_2$ emissions at 882Mt [3]. The sector is projected to grow with revenue passenger kilometres (RPK) doubling from approximately 2.5 trillion RPK in 2024 to near 5 trillion RPK in Europe by 2050 [4]. The growth in demand within the sector is projected to

have a significant increase in $CO_2$ emissions from current levels to approximately 2400Mt [5] without the intervention of strategic decarbonisation efforts, as seen in Figure 1.

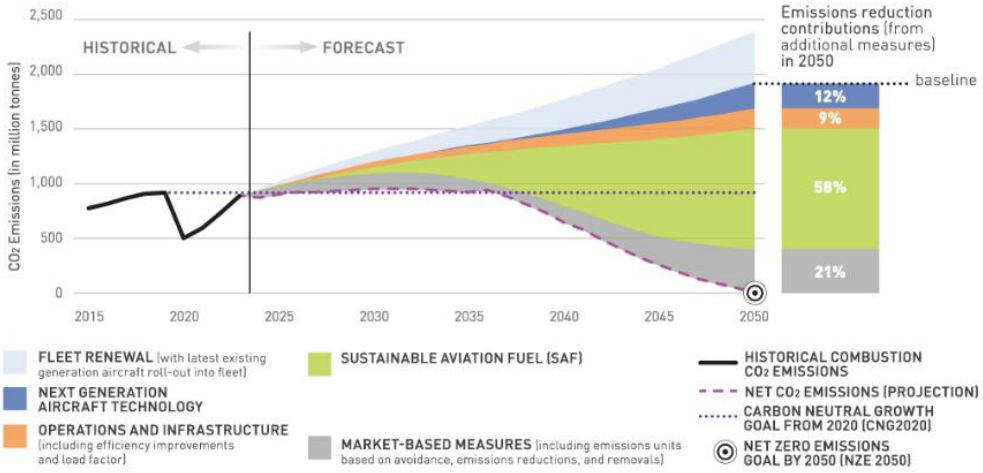



Figure 1: Projected increase in aviation's $CO_2$ emissions by 2050 [5]

The United Nations' Framework Convention on Climate Change (UNFCCC) held in 2015 led to the adoption of the Paris Agreement which seeks to hold the increase in the global average temperature to well below 2°C above pre-industrial levels and pursue efforts to limit the temperature increase to 1.5°C above pre-industrial levels [6]. The Paris Agreement therefore acts as the foundation and precursor for the aviation sector's decarbonisation efforts and reduction in greenhouse gas (GHG) emissions due their radiative forcing impact on the environment [7]. The sector has acknowledged its need to decarbonise with broad agreement across the sector's leaders that the decarbonisation effort must be multi-faceted and holistically viable. The International Air Transport Association's (IATA) Net -zero carbon 2050 resolution passed at the 77$^{th}$ IATA Annual General Meeting in 2021 outlined the need for the decarbonisation effort to comprise of advancements in technology, energy carriers, operations, finance and policy [8, 9]. The United Nation's (UN) International Civil Aviation Organisation (ICAO) commissioned the Long-Term Aspirational Goals (LTAG) report in 2022 at the 41$^{st}$ ICAO assembly and calls for the need of blended integration scenarios of operations, technology and fuel [10] with additional benefits to be leveraged from regulatory and policy-based measures [11]. Lastly, the Air Transport Action Group's (ATAG) Waypoint 2050 report foresees the decarbonisation of the sector being ushered in via scenarios of improved technology, operations, sustainable aviation fuel (SAF) usage and market-based measures [5]. The recurring and shared narrative amongst the sector's leaders that the decarbonisation of the aviation sector must be holistic in nature and broadly encompass focus on themes of technology, energy carrier, operations, market-based measures and policy demonstrates both the complex and comprehensive nature of the challenge. Therefore, analyses and investigations that reflect the holistic impact of decarbonisation concepts and assess their synergetic requirements from across the various factors, will provide the necessary clarity and characterisation of what is achievable from a sustainability perspective.

## 1.1 Literature Review

Alternative energy carriers are critical in reducing and negating the amount of $CO_2$ and other GHG emissions produced by the sector. SAF is an umbrella term used to describe energy carriers that act as substitutes for kerosene-based conventional aviation fuel, often via drop-in means (offering the lowest barrier to entry). As such, the production pathway of SAF is more sustainable and relies less on fossil-based, carbon-intense processes than conventional aviation fuel offering up to 80% reduction in WtW GHG emissions [12]. Hydroprocessed Esters and Fatty Acids (HEFA) is currently the most technically and commercially viable production pathway for SAF. It uses biomass waste as the source of carbon (hence, is referred to as bio-SAF), which are processed with hydrogen to create hydrocarbon compounds that form combustible fuel components viable for use in modern aeroengines [13]. Another SAF pathway is e-SAF, or Power-to-Liquid (PtL) SAF, which utilises renewable electricity to convert water into oxygen and hydrogen, then combines the hydrogen with a

$CO_2$ source via Fischer-Tropsch (FT) synthesis [14] to produce SAF [13]. Both SAF pathways offer significant reductions in carbon-intensity however, bio-SAF, while a viable pathway, competes with feedstocks and land-usage for other sectors' alternative energy sourcing in their own decarbonisation efforts limiting its scalability, especially in resource-restricted regions of the global sector. e-SAF requires renewable electricity sources which are not ubiquitously available, and production of e-SAF is a highly energy intensive process (production efficiency of 30.3% [15]). Hence, SAF offers promising reductions in emissions, but the viability of the respective production pathways are still uncertain with regards to scale and efficiency perhaps limiting their efficacy at decarbonising the sector. An alternative, low-carbon energy carrier which is not drop-in and requires significant aircraft specific and infrastructural re-configuration is liquid hydrogen ($LH_2$). Green $LH_2$ follows a similar pathway as the start of e-SAF whereby renewable electricity generates hydrogen and oxygen from water. This hydrogen is liquified by cooling it to cryogenic temperatures (-253°C) for use as an aviation fuel to be either combusted in traditional turbine engines or to power fuel cell propulsion architectures [16]. Depending on the carbon intensity of the electricity used in its generation, there are significant $CO_2$ emissions' reduction available from $LH_2$ use as an aviation fuel. However, the significant reconfiguration required of conventional aircraft to be powered by $LH_2$, a cryogenic fuel, leads to uncertain and shifted application of the alternative energy carrier.



Figure 2: NASA's N3-X electrified aircraft propulsion concept [16]

The regulatory components of the sector have been pursuing decarbonisation avenues too, such as the American Society for Testing and Materials (ASTM) approving 11 SAF production pathways to verify and validate the feasibility of different sustainable alternative, drop-in energy carrier options. The ASTM certification process verifies the originating pathway, feedstock option and blend limits, thus determining critical information for the production, distribution and consumption strategies that will be developed in the coming years to scale SAF consumption upwards and address $CO_2$ emissions via cleaner fuels [17]. In Europe, the ReFuelEU measure requires aviation fuel suppliers to gradually increase the supply of SAF in the sector through fuel blending with conventional aviation fuel. The ReFuelEU measure dictates that all EU airports must have a 70% share of SAF (half of which must come via the PtL pathway) by 2050, starting from 2% since 2025 [18]. These examples of the research and development activities from the stakeholders of the sector to target net-zero carbon emissions by 2050 convey a narrowed focus on decarbonisation of the aviation.

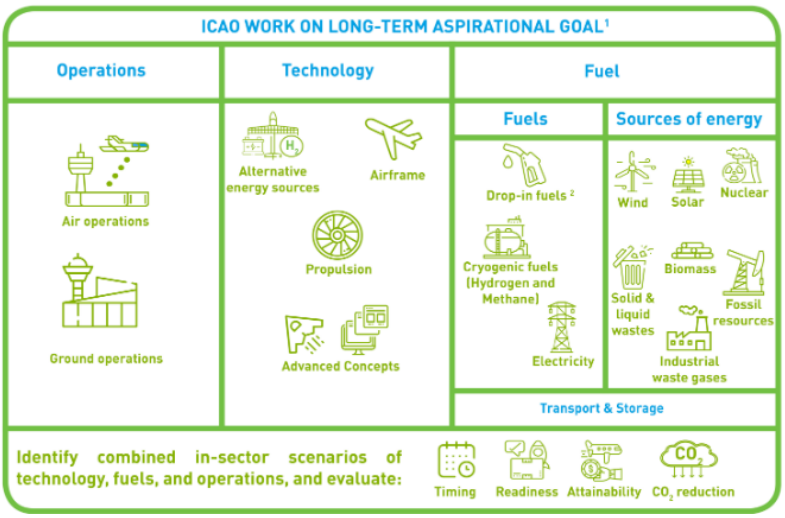



Figure 3 : ICAO's LTAG high-level overview of decarbonisation pathway [10]

With the plethora of decarbonisation advancements (and broad spectrum of avenues to investigate as seen in Figure 3), it is obvious that there is no single solution that will unilaterally result in the decarbonisation of this hard to abate sector. Secondly, a lot of the advancements are in technologies, energy carriers, operations and or policies which have not seen widespread adoption or application at present. The true extent of their decarbonisation potential cannot fully be validated until sufficient application of the research and development activities are seen within the sector. As such, research that can investigate the options the sector has and will have in the future, to explore how impactful they will be for interconnected deployment scenarios are critical undertakings as they link the design and application phases and assesses the decarbonisation potential accordingly. These types of investigations can provide the much-needed clarity in solution efficacy from a combined design and applications' perspective and aid in the decarbonisation pathways' decision-making process as a preliminary, exploratory framework. These studies could ask if what is being developed is addressing the problem through its design and application and make improvements as appropriate.

Airline scheduling models capture the application phase of a concept such that they select the way to operate a set of aircraft inside a network to move passengers through said network according to an objective function while being subject to logistical and feasibility constraints. Barzargan's "Airline Operations and Scheduling" sets out the fundamental methods behind scheduling an airline's operations [19]. The mathematics employ discrete optimisation methods, traditionally setting up the scheduling of operations as integer linear programming problems to be solved for maximised profit in resource constrained systems. The variables within these problems can be choices of route, passenger count, fuel allocations or aircraft type and are constrained by logistical and feasibility criteria. These constraints prevent physically impossible flight plans such as two or more departing flights from different airports being assigned to the same aircraft at the same time. The constraints also enforce or prevent behaviours such as maximum or minimum turnaround and downtimes for given aircraft. Through a non-traditional configuration of an airline schedule modelling where the scheduling is guided by sustainability rather than economic profit alone, the application phase of decarbonisation concepts may be analysed to advance or address the benefits or drawbacks, respectively. This style of scheduling model can provide insights into the efficacy of a decarbonisation concept during its application under a given decarbonisation pathway's scenario for the technology, energy carrier, operational, market and policy levels and thus, feedback design changes that improve its application and therefore the decarbonisation potential.

Utilising investigations which analyse the application phases for decarbonisation concepts through system-wide integration studies, technology utilisation assessments, market and policy understanding, and holistic optimisation approaches are therefore critical steps in taking technological advancements to real-world application. As seen by Roy et al. [20], who investigated a novel mixed-integer nonlinear programming methodology for designing an aircraft based on three core subspaces: "Aircraft Design Formulation", "Airline Allocation Formulation" and "Revenue Management Formulation". Roy et al. captured the operational strategy using a fleet allocation model and the economic performance of the airline with a revenue management model. The key result was that the aircraft designed, fleet allocated, and revenue acquired via the simultaneous optimisation of the design subspaces yielded a more profitable airline model. Maximising the revenue and minimising operating costs independently via the three-subspaces did not necessarily maximise the profit for the airline in these studies highlighting the need to investigate the technology, operations and market in a simultaneous, interconnected way.

Hoogreef et al. [21] investigated a "strategic airline planning model" which assessed and minimised an airline's climate impact based on the fleet planning and design of hybrid electric aircraft. This study conducted sensitivity analyses on the relationships between fleet composition and network planning with hybrid electric aircraft incorporated into the fleet. The study found that significant emissions reductions of 11% may be achieved when compared to the conventional aviation fuel fleet, but at the cost of 13% profit loss for the airline of the chosen design case. The study alludes to the imperative need to strategically implement specifically designed technology that has been informed by the operational nuances in which it shall be used, such that a breakeven or optimal operating-point can emerge where the benefits of maintaining or improving airline profitability can be achieved while simultaneously improving environmental sustainability. Championing either improved economic profit or reduced environmental impact to the detriment of the other is not a viable decarbonisation pathway.

The future of aviation will be built on sustainable business practices in an ever-decarbonising world, mandating the need for a synergetic harmony between economic and environmental viability.

Moolchandani et al. [22] discuss the creation of the Fleet-Level Environmental Evaluation Tool (FLEET) to assess the operations, economics and sustainability of an airline with the goal of tracking technologies' influence on aviation's pathway to decarbonisation. The FLEET framework utilises mixed-integer programming to represent the operational decision-making. The study investigates the relationship between technology and the $CO_2$ emissions of the aviation sector but delves into influencing factors outside of the technology itself. It was found that, given the expected advancements of technology in the future to render aircraft more fuel efficient by 2050, emissions will not reduce to the necessary levels without careful consideration of how airlines operate their aircraft within their networks, what energy carriers they rely upon, as well as how these may affect passenger demand and therefore the ability to generate profit within the sector. Again, the coupling of aircraft's performance and application were touched on when assessing the optimal pathway to decarbonising the aviation sector.

These studies within the literature demonstrate a trend whereby researchers are exploring the decarbonisation of the aviation sector from a more holistic, multi-faceted approach using discrete optimisation methods to guide their recommendations and claims for solutions to the net-zero challenge. It reflects the importance of having a well-rounded perspective on what leads to emissions within the sector and what mitigating measures can be developed to help reduce these emissions outside of, traditional technological advancement alone. Furthermore, the aggressive decarbonisation targets require revolutionary and disruptive changes to be made to the aviation sector. Prediction and evaluation models that do not rely wholly on historical data and trends alone but can objectively compare and decipher the true impact of decarbonisation pathways which are conceptual and deviate from the current modus operandi, will be crucial in providing the necessary confidence and inertia behind transitioning the sector to net-zero by 2050.

## 2. Methodology

The decarbonisation potential of alternative energy carriers is evaluated in this work by using a scenario evaluation framework which compares holistic sustainability performances for different operational scenarios. The evaluation framework uses a combination of aircraft performance data and discrete optimisation methods to simulate operational scenarios, assess the performance of the fleet, and therefore generate an objective basis from which comparisons of decarbonisation potentials may be derived. The objective basis for comparison is the holistic sustainability score of a given scenario. The holistic sustainability simultaneously evaluates the economic viability and environmental impact of the scenario, therefore maximising the holistic sustainability score is the equivalent of maintaining or increasing the economic viability while simultaneously decreasing the environmental impact relative to a competing scenario.

The sustainable aviation concepts created via the alternative energy carrier options to be explored in this work offer decarbonisation potential for the aviation sector through their reduction in Well-to-Wake (WtW) carbon-intensity (CI) relative to conventional aviation fuel, Jet A-1. However, the overall decarbonisation potentials of these concepts are dependent on five core themes: technology, fuel, operations, market and policy. While their WtW CI may be lower relative to Jet A-1, this fact alone may not be sufficient in justifying their use as a decarbonisation pathway for the sector. These alternative energy carriers will be influenced by all five of the themes, hence understanding and assessing the energy carriers along these themes will ultimately define the achievable decarbonisation potential from a holistic perspective. Along the technology theme, the aircraft specific in-flight performances will change due to aircraft design re-configurations to consume the specific fuel type. Along the fuel theme, the production, distribution and consumption pathways per energy carrier, with their associated environmental, economic and infrastructural needs will change. Along the operations theme, the turnaround logistics, connectivity of airports and ability to refuel aircraft will be impacted. Lastly, along the market and policy themes, the alternative energy carriers will have different fuel prices and emissions' penalisation levels, respectively. To truly evaluate how impactful these alternative energy carrier concepts are, a framework which evaluates their decarbonisation potential along all five of these core themes is essential.

## 2.1 Scenario Evaluation Framework

The framework used to investigate the various comparative studies later in this work is comprised of two sub-models: The "Aircraft Performance" and the "Scheduling" sub-models. The aircraft performance component of the framework encompasses a digital hangar of aircraft concepts, comprising conceptual design methods and predictions of concepts' in-flight performances across all feasible missions and the population of a database of these performance data – which is made available to the scheduling component of the framework. The scheduling sub-model handles the decision-making and running of the distinct operational scenario within the framework. The scheduling model produces a schedule of flights according to the scenario's definition for aircraft fleet, airport network, passenger traffic and decision weights, and finds the optimal set of flights for each aircraft that maximise the holistic sustainability score. As such, the framework enables the decarbonisation potential of the alternative energy carriers to be evaluated by firstly, simulating their conceptual aircrafts' performance capabilities and secondly, exploring the optimal application of such aircraft concepts inside operational scenarios.

### 2.1.1 Framework Overview

The use of the evaluation framework follows a two-part process: firstly, the aircraft performance database for the concepts are populated with all feasible missions and their associated in-flight performances (fuel consumptions and emissions). Secondly within the scheduling component, the operational scenarios are defined, the aircraft concepts' data are shared and optimal holistically sustainable schedules per scenario are determined for the purpose of comparative analysis of the decarbonisation potentials.

*Design – Aircraft Performance*

The baseline aircraft used in this analysis was the 197 seat, CFM-LEAP-1B27 powered, Jet A-1 fuelled, B737-8200 MAX aircraft, henceforth referred to as the conventional MAX or conv. MAX. Two alternative energy carrier variants were designed as reconfigurations of the conv. MAX's airframe to account for the cryogenic nature of the LNG/RNG and $LH_2$ fuels. These alternative fuel variants are referred to as the NG MAX and $LH_2$ MAX for the LNG/RNG and $LH_2$ fuelled variants, respectively. A previously existing database for the conv. MAX aircraft's performance predictions was produced in the work by Barry et al. [23, 24] and validated using real-world flight data of 1706 flights from Ryanair's operations. The same aircraft performance model to be discussed in this section was used in these works and produced performance predictions for the conv. MAX with a mean fuel burn error across the payload-range operating envelope of 5.87%. Similarly, the modelling framework developed by Gallagher et al. [25] was used to reconfigure the airframes to create the NG MAX and $LH_2$ MAX aircraft for analysis in this work. The aircraft performance model follows the flowchart shown in Figure 4.

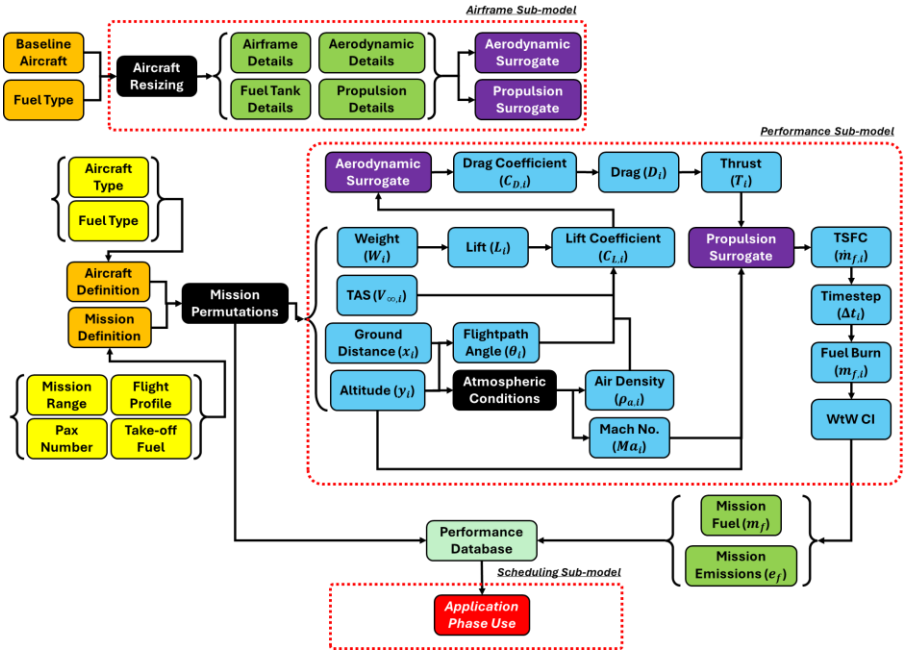



Figure 4: Aircraft Performance component of framework flowchart

Firstly, to generate the LNG/RNG and $LH_2$ fuelled aircraft concepts, the base aircraft was resized to account for inclusion of fuselage mounted cryogenic fuel tanks (further detail is provided in the coming paragraphs). The sizing was conducted on the basis of maintaining the same top level aircraft requirements (TLARs) as the base aircraft (passenger capacity, cruise Mach and design mission range), in addition to the need to service an EASA CS-25 certified reserve mission [26, 27]. This reserve mission was deemed to be a critical inclusion to ensure that the different energy carriers could be compared on a like-for-like basis, while maintaining the same network capacity in terms of available seat kilometres (ASKs). Additionally, due to the cryogenic nature of the LNG/RNG and $LH_2$ fuels, the wing masses were increased by 3.42% [28] to account for structural reinforcing of the dry-wing, alternative energy carrier concepts. These requirements and parameters were supplied to the aircraft airframe sub-model produced by Gallagher et al. [25] utilised for aircraft resizing, the methodology of which is shown in Figure 5. The outputs from this component were the details regarding the airframe size (fuselage length, wetted areas, etc.), fuel tank capacity, operating empty weight (OEW) and a set of lift versus drag coefficients to characterise the aerodynamics and drag performance of the reconfigured aircraft. The outputs from this sub-model are stored in aerodynamic and propulsion surrogates for use in the next part of the performance model.

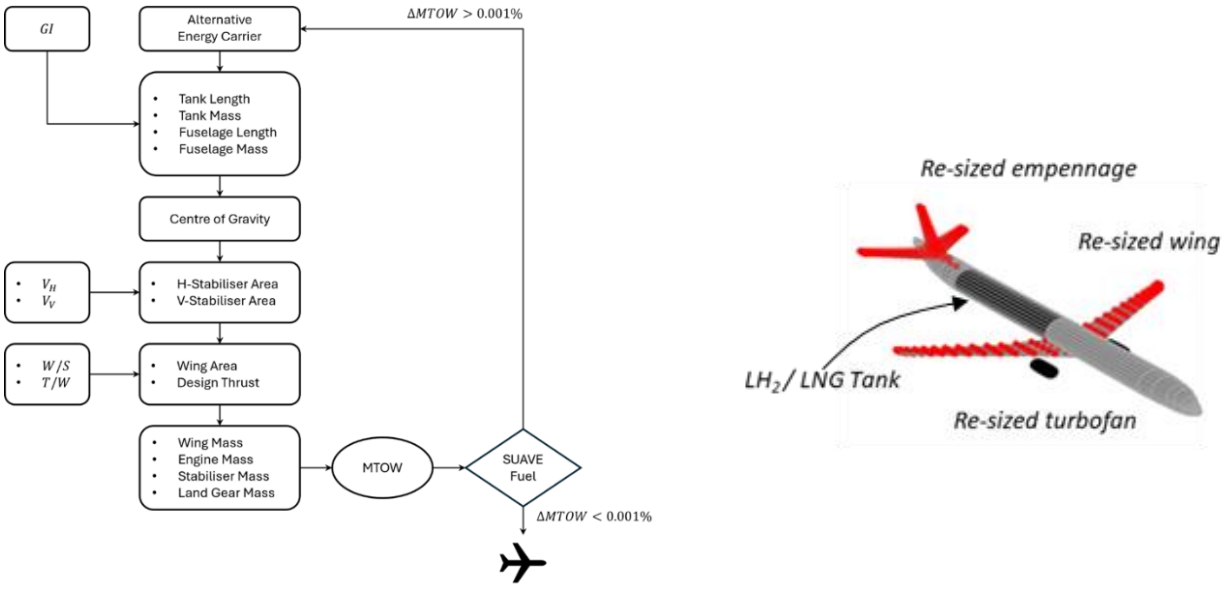



Figure 5: Overview of aircraft sub-model iterative sizing process, alongside a sample conceptual aircraft design

The aircraft and mission definitions are then supplied to the performance sub-model developed in Barry et al. [23, 24] to generate the mission permutations and calculate all fuel consumptions and emissions associated with each mission. Firstly, the weight ($W$), true airspeed (TAS, $V_\infty$), ground distance ($x$) and altitude ($y$) values for each segment along the flight profile (denoted by the $i$ subscript) are set, the weight is initialised as the take-off weight (TOW) and deceases based on the amount of fuel consumed per segment. With the ground distance and altitude covered in the segment known, the flight path angle ($\theta$) is calculated by Equation (1) which enables the determination of the lift ($L$) required to overcome the weight of the aircraft, as seen by Equation (2).

$$tan\theta_i = \frac{y_i - y_{i-1}}{x_i - x_{i-1}} \quad (1)$$

$$L_i = W_i \cdot cos\theta_i \quad (2)$$

The altitude and TAS enables the calculation of the air density ($\rho$) and Mach number (henceforth referred to as Mach No. and given by the symbol $Ma$) using NASA's standard atmospheric model [29]. Knowing the required lift, air density, wetted area (given per aircraft type, $S_w$) and TAS, the lift coefficient ($C_L$) is calculated, as seen in Equation (3).

$$C_{L,i} = \frac{L_i}{0.5 \cdot \rho_i \cdot S_w \cdot V_{\infty,i}^2} = \frac{2 \cdot W_i \cdot cos\theta_i}{\rho_i \cdot S_w \cdot V_{\infty,i}^2} \quad (3)$$

sThe aerodynamic surrogate relates the lift to the drag coefficients ($C_D$) via a parabolic drag polar, as seen in Equation (4), where the $k$ and $C_{D,0}$ fitting parameters are determined from the airframe sub-model of Gallagher et al. [25]. This aerodynamic surrogate gives a value for the drag coefficient based on the supplied lift coefficient which is then used to calculate the drag ($D$) via Equation (5).

$$C_{D,i} = C_{D,0} + k \cdot C_{L,i}^2 \quad (4)$$

$$D_i = 0.5 \cdot C_{D,i} \cdot \rho_i \cdot S_w \cdot V_{\infty,i}^2 \quad (5)$$

Knowing the drag, the required thrust ($T$) to overcome this drag during the segment can be calculated according to Equation (6). This required thrust, in conjunction with the values for the Mach No. and altitude are supplied to the propulsion surrogate to determine the associated thrust specific fuel consumption (TSFC) via a lookup table, shown in Equation (7). This TSFC value is converted from a rate of fuel consumption ($\dot{m}_{f,i}$) to a mass of fuel consumed ($m_{f,i}$) by integrating the consumption rate over the timestep taken to complete the segment ($t_i$) of the flight profile, as shown in Equation (8).

$$T_i = D_i - W_i \cdot sin\theta_i \quad (6)$$

$$TSFC_i = func(Ma_i, y_i, T_i) = \dot{m}_{f,i} \quad (7)$$

$$m_{f,i} = \int \dot{m}_{f,i}\, dt_i \quad (8)$$

This weight of fuel consumed during the segment (product of mass and acceleration due to gravity, $g$) is recorded and deducted from the total aircraft weight prior to the next calculation loop for the next segment, shown in Equation (9). However please note, when using alternative energy carriers (not Jet A-1), the mass of fuel consumed per segment is converted to an amount of energy consumed via the lower-heating value (LHV) of Jet A-1, 43.3MJ/kg [30], then converted to an energy-equivalent amount of mass of the alternative fuel (denoted by the $alt$ subscript) via the LHV of the other fuel. This is shown in Equation (11) where the mass of fuel consumed per segment for alternative energy carriers ($m_{f,alt}$) is equal to the product of the calculated value for the mass of consumed fuel from the propulsion surrogate ($m_f$) and the ratio of the LHVs between the fuel types ($\mu_{LHV}$).

$$W_{i+1} = W_i - m_{f,i} \cdot g \quad (9)$$

$$\mu_{LHV} = \frac{LHV_{Jet\ A-1}}{LHV_{alt}} \quad (10)$$

$$m_{f,alt,i} = m_{f,i} \cdot \mu_{LHV} \quad (11)$$

All the segmental fuel consumptions are summed across the total flight profile to determine the mission fuel consumption ($m_{f,m}$) and the WtW $CO_2$ emissions ($e_{f,m}$) associated with the given mission permutation using the WtW CI ($CI$) and LHV of the fuel, as seen in Equations (12) and (13).

$$m_{f,m} = \sum m_{f,i} \quad (12)$$

$$e_{f,m} = CI \cdot m_{f,m} \cdot LHV \quad (13)$$

The mission permutations and their specific performances are recorded and populate the performance database which are later used in the scheduling component of the framework. Figure 6 is a visual representation of the fuel consumption data which populates this resultant “Performance Database” block at the bottom of Figure 4. The tri-variate missions are denoted by their choice for mission range, passenger allocation and fuel level at take-off and have their associated mission fuel

consumption indicated by the normalised colour contour. This database informs the scheduling component of the exact cost a given mission decision has from a fuel consumption and emissions perspective for each aircraft type under analysis within the framework.

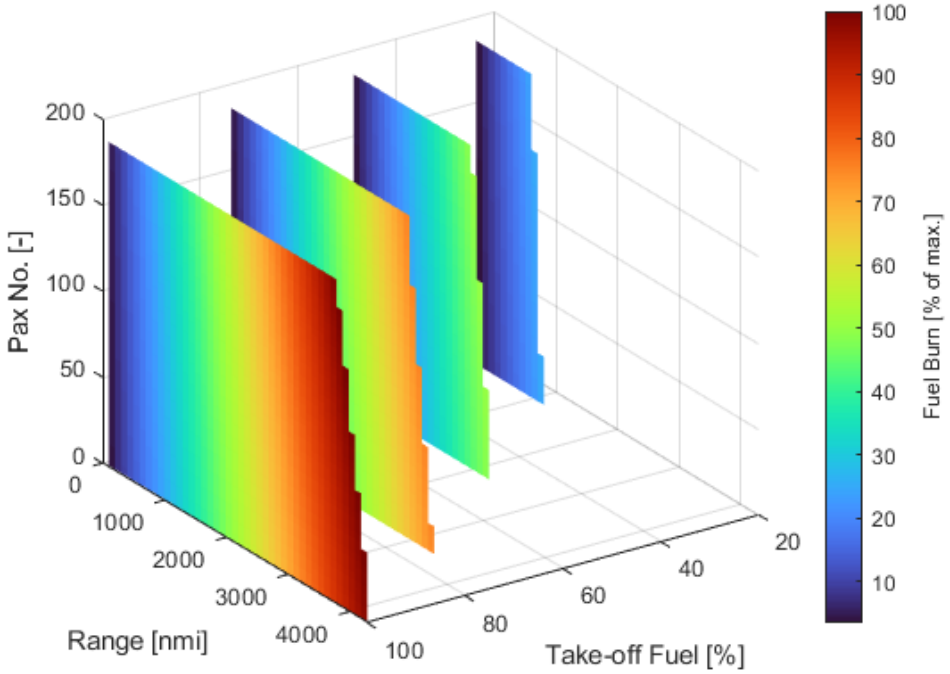



Figure 6: Tri-variate mission specific fuel consumption contour plot of a conv. MAX aircraft

While the aircraft performance sub-model can evaluate aircraft concepts' performances for all feasible missions, the aircraft concepts studied in this work only consider a restricted set of missions for the purpose of isolating differences in holistic sustainability performance to the variation in energy carrier. This restriction in missions is that the take-off fuel variable is fixed such that aircraft always land with enough fuel to complete the EASA CS-25 reserve mission [26, 27]. Hence, with known mission fuel consumptions and by using the aircraft performance sub-model to determine the amount of fuel the reserve mission requires per aircraft type, the required take-off fuels for each combination of passenger and range for each MAX variant can be determined. This functionality is denoted by the constraint relating take-off fuel ($f_{TO}$), mission fuel ($f_M$), reserve fuel ($f_R$) and landing fuel ($f_L$) in Equation (14).

$$f_{TO} = f_M + f_R \rightarrow f_L = f_R \tag{14}$$

The NG MAX and $LH_2$ MAX aircraft both use cryogenic fuels which require the reconfiguration of the base airframe to a dry-wing, fuselage-based fuel tank compared to the wing-based fuel tanks of the conv. MAX. The resizing of the NG MAX and $LH_2$ MAX aircraft within the airframe sub-model from Figure 4 and Figure 5 are guided by adjusting the design of the aircraft to being fuelled by LNG/RNG and $LH_2$ for the NG MAX and $LH_2$, respectively. At the same technology level, these fuels have different attainable gravimetric indices (GI) for their fuel tanks. The TLARs of airframe and propulsor technology levels, design mission, reserve mission and deliverable ASKs are fixed across the conv. MAX, NG MAX and $LH_2$ MAX to isolate changes in each variants' sustainability performances and operability to the alternative energy carrier alone. Hence, all resulting changes to the airframe are due to the difference in GI of the fuel tanks and fuel properties while maintaining all other TLARs. The GI of the NG MAX and $LH_2$ MAX fuel tanks are 83% and 45% [31], respectively and are set as such based on the expected technology readiness level (TRL) for these fuel types by 2035. Table 1 and Figure 7 convey some indicative design data and the drag polars for each airframe, respectively, to highlight the changes, and ultimately demonstrate the shift in performance from using alternative energy carriers with the given TLARs.

Table 1: Differences in key airframe design data across MAX variants

| *Parameter* | *Conv. MAX* | *NG MAX* | *$LH_2$ MAX* |
|---|---|---|---|
| Fuel Options | Jet A-1, SAF | LNG, RNG | $LH_2$ |
| Cryo-tank GI (%) | - | 83 | 45 |
| Fuselage Length (m) | 39.12 | 46.70 | 59.46 |
| OEW (kg) | 44045 | 56824 | 81818 |
| Reserve Fuel Req. (% of max. tank vol.) | 13.08 | 14.38 | 17.34 |

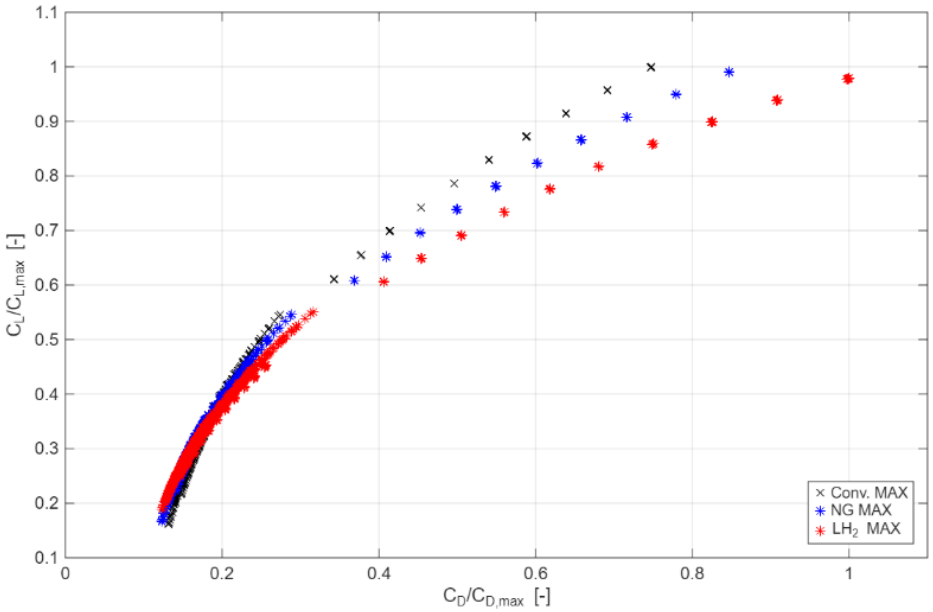



Figure 7: Normalised drag polar comparisons across MAX variants

The alternative energy carriers impact the MAX aircraft design by increasing the fuselage length, wing area and OEW which reduce the aerodynamic efficiency of the airframe relative to the conv. MAX. As seen in Figure 7, the NG MAX and $LH_2$ MAX have a higher drag coefficient (with the $LH_2$ MAX being consistently worse) for every lift coefficient compared to the conv. MAX. This produces an increased in-flight energy demand for the NG MAX and $LH_2$ MAX aircraft relative to the conv. MAX aircraft when completing the same mission. As seen by Equations (1) to (13) above, the fuel consumed per mission is a function of the incremental fuel consumptions which are in turn a function of the aircraft weight and aerodynamic characteristics per segment. As can be seen in Table 1, the amount of fuel required to complete the same reserve mission increases when using the alternative energy carriers. The heavier, less aerodynamically efficient NG MAX and $LH_2$ MAX therefore suffer a higher in-flight energy penalty when operating the same missions as the conv. MAX.

The productivity specific energy consumption (PSEC), as shown in Equation (15), is the ratio of the energy consumed from the mission fuel ($E_{cons}$) to the energy-equivalent of the revenue passengers flown ($E_{RPK}$). The energy-equivalent of passengers flown is equal to the product of the number of passengers ($n_p$), an average passenger mass ($\bar{m}_p$), acceleration due to gravity and the distance flown ($d_m$). This non-dimensional metric conveys the energy efficiency of aircraft completing missions within a network where flying passengers to their destination is the measure of productivity. As such, relatively lower PSEC values indicate more efficient use of the consumed energy to fly passengers along a given route whereas higher PSEC values indicate sub-optimal performances from a consumption and or productive perspective. The PSEC performances across all mission range and passenger count combinations of interest to this study are shown for the conv. MAX, NG MAX and $LH_2$ MAX in Figure 8, Figure 9 and Figure 10, respectively.

$$PSEC = \frac{E_{cons}}{E_{RPK}} = \frac{m_{f,m} \cdot LHV}{n_p \cdot \bar{m}_p \cdot g \cdot d_m} \quad (15)$$

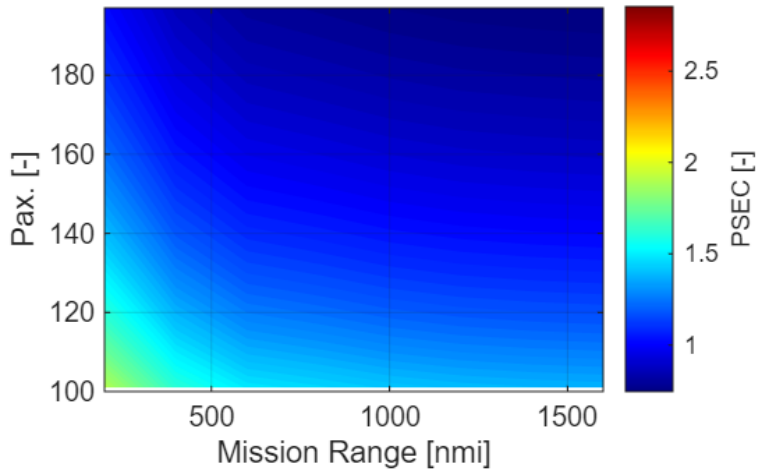



Figure 8: PSEC across mission permutations for the conv. MAX

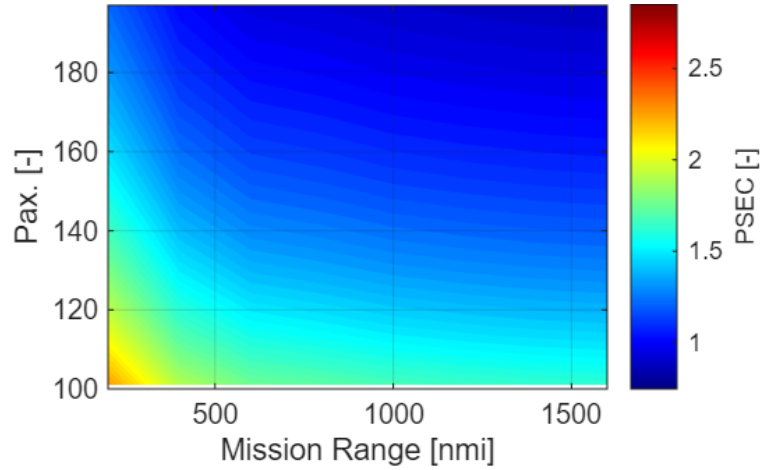



Figure 9: PSEC across mission permutations for the NG MAX

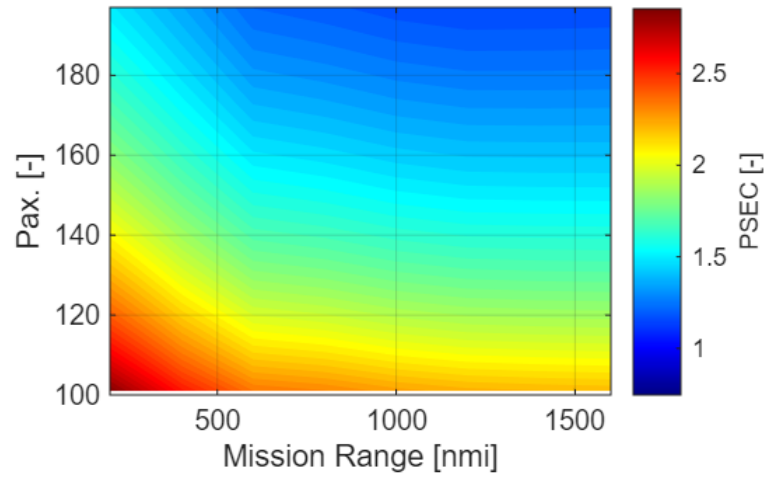



Figure 10: PSEC across mission permutations for the $LH_2$ MAX

Table 2: Load-factor averaged in-flight (TtW) energy penalties relative to the conv. MAX

| ***Mission Range (nmi)*** | ***NG MAX Penalty (%)*** | ***$LH_2$ MAX Penalty (%)*** |
|---|---|---|
| 200 | +18.30 | +50.24 |
| 600 | +18.38 | +58.66 |
| 1000 | +18.44 | +59.97 |
| 1400 | +18.91 | +60.18 |

As illustrated in Figure 8, Figure 9 and Figure 10, and shown by the data of Table 2, the NG MAX and $LH_2$ MAX suffer higher in-flight energy consumption penalties relative to the conv. MAX due to the airframe reconfigurations to account for the cryogenic, fuselage-based fuel tanks. This in-flight performance penalty is highlighted by the PSEC values for the NG MAX and $LH_2$ MAX being worse than the conv. MAX for all possible missions when comparing Figure 9 and Figure 10 to Figure 8. Similarly, the energy penalty associated with using the alternative variant MAX aircraft can be seen by the relative increase in the load-factor averaged energy consumptions per mission range in Table 2. The $LH_2$ MAX is the most impacted by the decrease in performance with the highest of the PSEC values and worst relative increase in average energy demand across the three MAX variants (as bad as a 60.18% increase in energy demand relative to the conv. MAX on the longest ranged routes). While the NG MAX suffers an energy penalty relative to the conv. MAX, it has only a moderate increase in energy penalty values compared to the severe impact in performance of the $LH_2$ MAX.

### *Application – Scheduling*

The scheduling component of the framework acts as the decision-making branch of the overall architecture. By curating operational scenarios and supplying accurate performance data for the decarbonisation concepts via the previously discussed aircraft performance sub-model, the scheduler can objectively assess the potential of the scenario by choosing the best set of decisions. Then by comparing the optimal schedule produced for a given scenario to other operational scenarios' schedules with variations in the decarbonisation levers therein, the overall sustainable aviation design space can be characterised and operationally viable decarbonisation pathways discovered. The modelling of an operational scenario within the scheduling pillar encompasses five stages: Inputs, Variables, Constraints, Objective and Solution. These sequential stages define, construct and solve the problem space generated by the operational scenario and are curated by the investigating decarbonisation pathways' options and levels for the core themes of technology, energy carrier, operations, market-based measures and policy. A detailed description of the scheduling sub-model's development and the mathematical methods employed therein are discussed in prior work by Barry et al. [32] however, a summary of the scheduling component's methodology and workflow is portrayed in Figure 11.

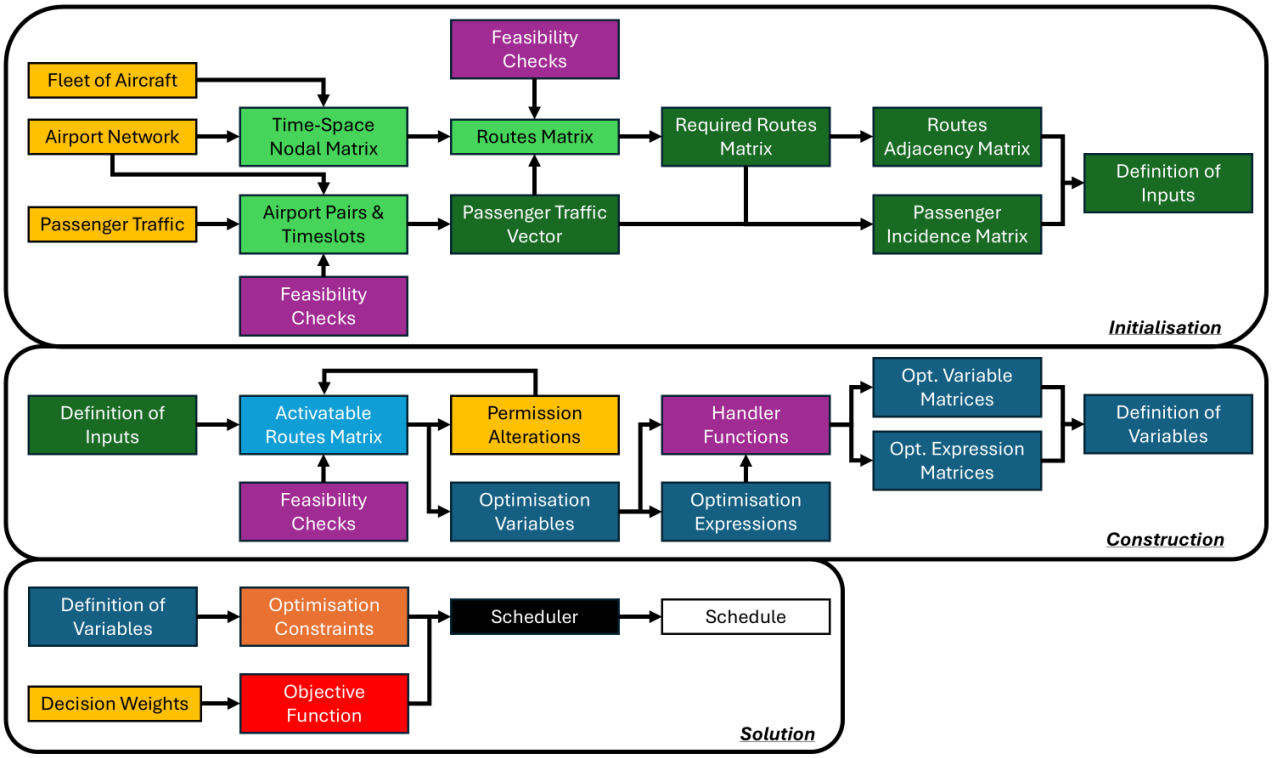



Figure 11: Scheduling sub-model flowchart

The "Initialisation" block defines the inputs to the scheduling sub-model and curate the design space according to the five decarbonisation themes of technology, energy carriers, operations, market-

based measures and policy. The inputs for the fleet of aircraft describe the decarbonisation level offered by the technology and energy carrier themes of the scenario, i.e the different aircraft designs, the types of performance improvements and the types of fuel used to power them with the associated emissions all being modelled in the aircraft performance sub-model previously discussed. The fleet of aircraft input is informed by the performance sub-model's "Performance Database" block from Figure 4 and acts as the data-transfer connection between the two sub-models. The airport network and passenger traffic input defines the operations theme of the decarbonisation scenario under investigation, i.e the connectivity of the network, the availability of fuels, the timeslots, the turnaround logistics as well as the when, where and how many people want to travel through the network. Lastly, the decision weights (which feeds into the "Objective Function" at the bottom of Figure 11) defines the decarbonisation level of the market-based measures and policy themes. The decision weights assign the objective advantages and drawbacks associated with each decision that can be made in the model, i.e the amount of revenue generated from flying a number of passengers on a given route less the operating costs incurred due to fuel costs, crew costs, landing and handling fees and the $CO_2$ emissions' penalisation. The market-based measures and policy themes are defined here as pricing/cost levels and emissions penalisation levels, respectively. Therefore, each decision, an allocation of a mission to an aircraft within the schedule, will have specific impacts on the revenue generation, cost accrual and penalisation amount of a given scenario's schedule. Hence the scheduler is tasked with determining optimal mission sets given these inputs for the decarbonisation themes of technology, energy carrier, operations, market-based measures and policy.

The "Initialisation" block culminates with a definition of the scenario to be investigated and poses it as a mixed-integer linear programming (MILP) problem where the inputs define variables, constraints and an objective function such that the scheduler (solver of the MILP problem) must find an optimal schedule of flights to maximise the holistic sustainability score of the scenario. The "Construction" block generates mathematical relationships for the inputs and the variables such that a logical design space can be explored and optimised. The optimisation variables, the decisions the scheduler can make for the given scenario to optimise the schedule, are the choice of route, passenger number and fuel allocation for all aircraft supplied within the aircraft fleet input. The "Construction" block, after curating a MILP problem and defining the variables for scheduling, connects to the "Solution" block which defines constraints based on these variables alongside constructing the objective function to determine an optimal solution. The constraints handle the feasibility and logic enforcement of the schedule. For brevity, not all constraints used within the model will be discussed as a detailed description of each constraint can be found in the prior, developmental work of Barry et al [32], however some high level constraints and their purpose will be mentioned. Logical constraints such as spatial and temporal adherences exist for the allocation of flights. Spatially, an aircraft's second flight cannot depart from a different airport to its first flight's arrival airport, i.e all aircraft must depart from the same airport as where they landed immediately prior. Temporally, an aircraft cannot be assigned a departure time for a flight prior to completing its landing and turnaround of the preceding/current flight, i.e the departure time of the succeeding flight must be operationally feasible with regards to the preceding flight's arrival and turnaround time requirements. These constraints enforce the allowable values of the optimisation variables and restrict illogical and non-sensical schedules from being generated or explored. Other constraints exist with regards to routing and chaining of flights which are handled by connectivity matrices such as the "Activatable Routes Matrix" in Figure 11. These matrices enable feasibility checks across the design space to ensure logical sequencing of flights and enable the schedule to assign superior flight plans to each aircraft such that an optimal, fleet wide schedule of flights be created.

The model uses a single objective function defined as the holistic, hybrid economic and environmental sustainability metric that ranks the optimality of a given schedule succinctly with units of currency. The input information of the previously mentioned decision weights guides the optimisation of the schedule by determining the objective function's value. The decision weights are the user defined objective values associated with each decision that can be made in the model, i.e the revenues, costs and emissions' penalties associated with each choice. These decision weight matrices are defined in Table 3. The objective function is designed to maximise the hybrid sustainability of the schedule. This hybrid sustainability is expressed solely in terms of currency by measuring traditional economic profit (all revenues less all costs) less the environmental impact (amount of emissions) converted into units of currency via emissions' penalisation conversion metrics.

Table 3: Decision weight matrix breakdowns

| *Name* | *Symbol* | *Units* |
|---|---|---|
| Base Passenger Revenues | $\phi_{p,b}$ | € |
| Distance Passenger Revenues | $\phi_{p,d}$ | €/RPK |
| Landing Costs | $\phi_L$ | € |
| Handling Costs | $\phi_H$ | € |
| Crew Costs | $\phi_C$ | €/min |
| Fuel Costs | $\phi_F$ | €/L |
| Emissions' Costs | $\phi_E$ | €/kg of $CO_2$ |

Through revenues, costs and currency valued $CO_2$ emissions' penalties, the objective function captures the impact on economic behaviour and the environmental performance of the schedule and outputs a single, holistic sustainability metric ($\gamma$) with units of currency where higher objective values indicate stronger performing schedules. The objective function is defined as the revenue from passengers ($\alpha_p$) less the costs of landing ($\beta_L$), handling ($\beta_H$), crew ($\beta_C$), fuel ($\beta_F$) and emissions ($\beta_E$). Passenger revenue depends on the aircraft, route selected (where longer routes have a distance weighted increase in pricing) and the number of passengers flown. Landing and handling costs depend on the airport and type of aircraft. Crew costs depend on the type of aircraft and time active. Fuel costs depend on the type of aircraft, energy carrier and refuelling airport. Emissions' costs depend on the type of aircraft and the emissions' penalisation conversion metric used, the EU emissions' trading system (ETS) penalisation structure for example [7]. It is these parameters in Table 3 that act as the weightings against the decision variables in the objective function. It can therefore be understood that tuning these weighting parameters between runs of the same scenario can produce substantially different solutions. This tuning is controlled by the user to curate a preset scenario for a certain technology's cost, energy carrier's cost, emissions' penalty level, or other decarbonisation levers.

$$\gamma = \alpha_p - (\beta_L + \beta_H + \beta_C + \beta_F + \beta_E) \tag{16}$$

### 2.1.2 Framework Validation Scenario Definition

The validation of this decarbonisation scenario evaluation framework uses real-world data from the industrial collaborator, Ryanair DAC. The validation involves the running of the model with real passenger traffic data in a real network of airports using performance predictions based on real aircraft (the conv. MAX aircraft as discussed in Section 2.1.1). A network of ten European airports, comprising 72 distinct routes was input to the scheduling sub-model with Ryanair passenger data from 22nd December 2025. The ten airports, denoted by their IATA codename, were STN, DUB, BGY, BCN, CRL, BVA, FAO, BER, KRK and ATH. The first five airports of this list are the five most served airports by Ryanair [33] with the remainder of the airports having high volumes of passenger traffic from these first five and thus, creating a strongly connected network to test the scheduling capabilities of the framework. The airport network and normalised passenger traffic used in this scenario are visualised in Figure 12 and Figure 13, respectively. Please note that each of the red-dotted lines connecting airports in Figure 12 count as two separate routes within the mathematical representation of the model. For example, the red-dotted line connecting DUB and FAO airports creates the routes DUB-FAO and FAO-DUB to distinguish between where passengers enter and exit the network. Secondly, as the passenger data supplied to the framework is for a single day of operations across the relevant airports, the scheduling sub-model is set to an operating window of a single day.

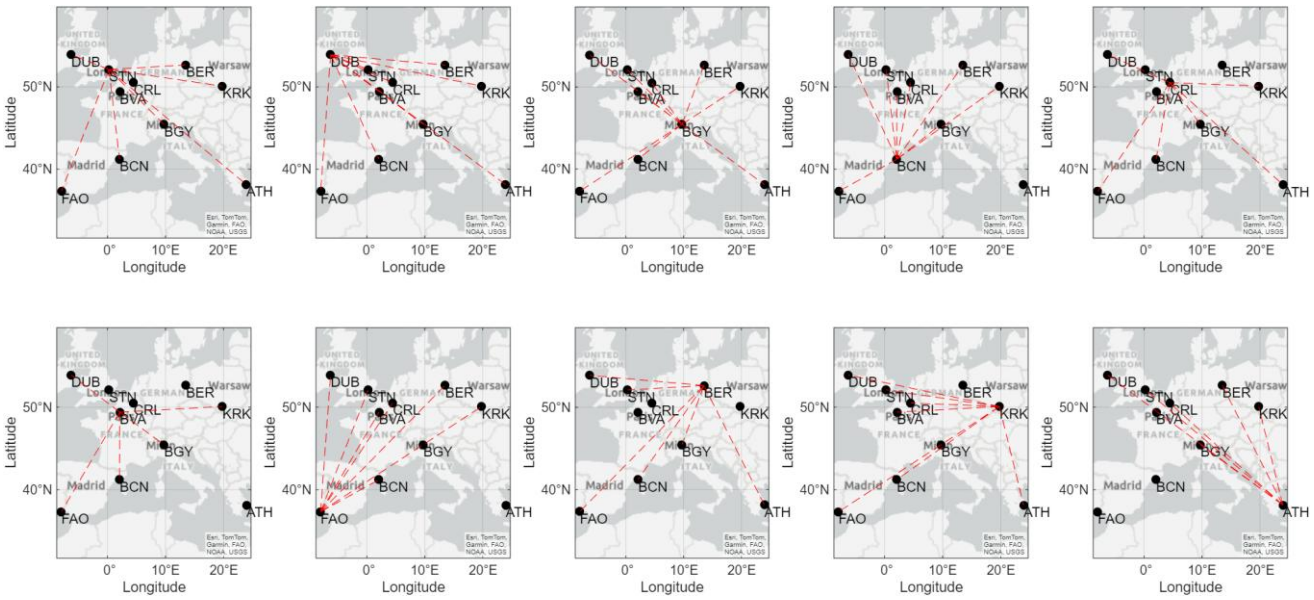



Figure 12: Airport network with airport specific routing options per plot




Figure 13: Normalised passenger traffic route-specific (airport pairs) heatmap

Not all of the values for the decision weights used in this analysis can be divulged due to data-sensitivity reasons. These are namely the values for the decision weights assigned to the passenger revenue, crew costs, landing and handling fees. However, all these decision weights are held constant throughout all analyses in this work, hence differences between the comparative scenarios' results to come are due to the differences in the publicly available values of the weights for fuel costs and emissions' penalties and the different performances of the aircraft under investigation. For the validation scenario, the fuel cost for Jet A-1 was set at €0.50/L [34] and the $CO_2$ penalty level was set as €70/1000kg of $CO_2$ due to EU ETS' current (2026) carbon tax [7]. This validation scenario is the simulation of the current (2026) fleet (all conv. MAX aircraft fuelled 100% by fossil Jet A-1) operating in the above airport network with the above passenger traffic. The validation scenario's simulation resulted in 97.3% of the total real-world passenger traffic being allocated to flights by the scheduling sub-model showing strong capture of the necessary functionality, as seen in Figure 14.

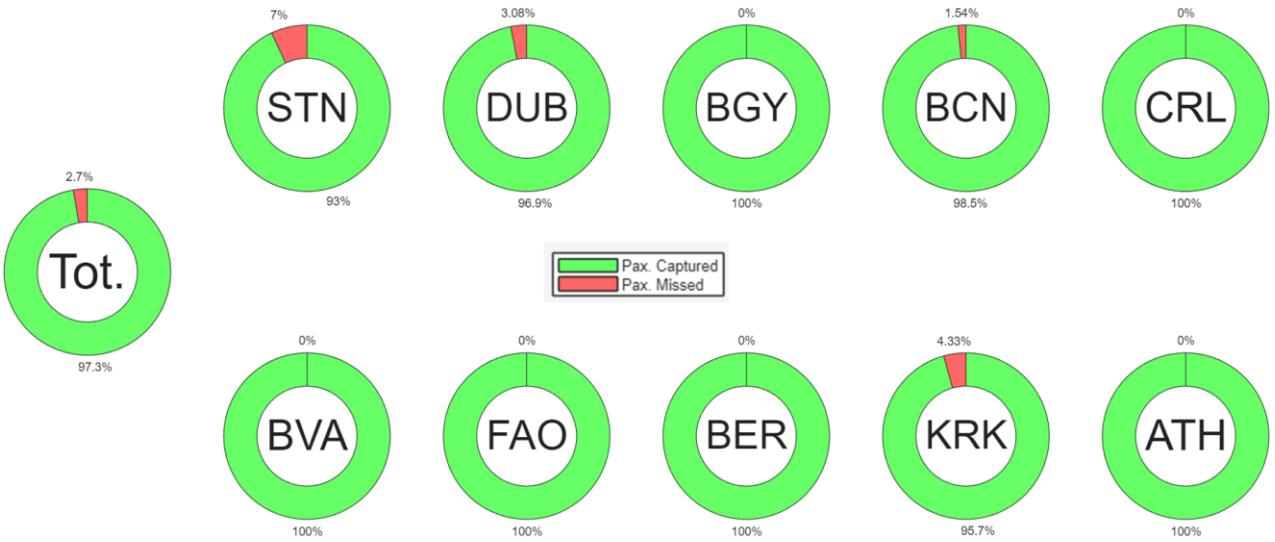



Figure 14: Total ("Tot.") and departure airport breakdown of passenger traffic capture

The mathematical constraints used within the scheduling sub-model of the framework cannot be broken for any flights or missions allocated by the scheduler. The operational scenario, as defined by the inputs, does not change while the scheduler is running, hence the output schedule is an optimal set of decisions for that specific day of operations and reflects no stochastic or unexpected changes to that scenario across the operating window as the schedule is complete. However, real-world schedules must adapt to these stochastic and unexpected changes to operations as an operating period is completed. Stochastic variables such as weather or engineering issues have knock-on effects on aircraft availability within a flight plan such that aircraft are assigned to different flights than originally planned which may breach logistical constraints such as an aircraft being required to complete a return to original base (RTB) flight at the end of the day, which is present in the simulation framework. The real-world schedule can adapt its flight plans live to allow a once-off or select few flights to breach this constraint such that the impacted passengers are captured and revenue generated. However, the deterministic nature of the framework's scheduling sub-model with an assumption of the scenario's passenger traffic and aircraft availability being fixed at the outset of the problem does not permit this constraint suppression and therefore leads to slight discrepancies (2.7%) between the simulated and actual passenger capture. The 2.7% passenger non-capture are passengers which were flown on the remainder flights between the airports that have sub-100% passenger captures (STN, DUB, BCN and KRK as seen in Figure 14) which are flights that breached this RTB constraint in reality but were catered to due to live schedule adaption. The framework could not find a logical flight plan (feasible sequence of flights) for an aircraft to cater to these passengers across these airports while adhering to the RTB constraint, hence the accumulated 2.7% reduction in passenger service may be attributed to stochastic discrepancies between simulated and real-world flight scheduling capabilities. Lastly, Ryanair claimed a profit of €2.26 billion serving 200.2 million passengers in 2025 [35], achieving a profit per passenger of €11.23/pax. The profit per passenger achieved for the scheduling sub-model was €11.41/pax for the validation scenario therefore faithfully representing the real-world operations.

## 2.2 Baseline 2035 Scenario Definition

The baseline 2035 scenario is compared to the previously shown 2026 validation scenario. The purpose of defining, then comparing the baseline 2035 scenario to the present day (2026), validation scenario is to demonstrate that the landscape of the aviation sector will change with time even if alternative energy carriers are not pursued. This is due to the 2035-timeframe policy and market-based measures such as ReFuelEU [18] and EU ETS [7] implementing mandatory levels of SAF blending and emissions' penalty increases, respectively.

Like the validation scenario, the baseline 2035 scenario's fleet is 100% conv. MAX aircraft, and the network and passenger traffic inputs remain unchanged. However, now the conv. MAX are fuelled with a blend of 80% fossil Jet A-1, 15% bio-SAF and 5% e-SAF, as governed by ReFuelEU [18]. Henceforth, the 2035 baseline's fuel blend will be referred to as "80/20 C/SAF" due to its 80%

conventional fuel and 20% SAF split in composition. Furthermore, the $CO_2$ emissions' penalty level increases between the validation and baseline 2035 scenarios going from €70/1000kg to €200/1000kg of $CO_2$ as governed by the EU ETS framework [7]. Firstly, through the use of SAF blending, the WtW CI of the 2035 baseline scenario's fuel decreases from 89g$CO_2$/MJ to 76.125g$CO_2$/MJ based on a fraction-weighted average of the WtW CI of the comprising fuel strands, as shown in Equation (17). The CI of Jet A-1, bio-SAF and e-SAF are 89g$CO_2$/MJ [36], 27.3g$CO_2$/MJ [37] and 16.6g$CO_2$/MJ [37], respectively. Secondly, two versions of the baseline 2035 scenario are compared to the validation scenario to upper and lower bound the degree of change in sustainability performance by 2035. These upper and lower bounding versions are the minimum cost (best-case) and maximum cost (worst-case) scenarios for fuel pricing, respectively. All other parameters within the best- and worst-case versions of the baseline 2035 remain constant except for the prices of the 80/20 C/SAF fuel (minimum and maximum) which are determined similarly to the CI, on a fraction-weighted average, as shown in Equation (18). The price of Jet A-1 remains constant as before at €0.50/L, whereas the prices of bio-SAF [38] and e-SAF [39] are set at €1.00/L and €1.00/L, or €1.25/L and €2.00/L for the minimum and maximum price versions of the baseline 2035 scenario, respectively.

$$CI_{80/20\ C/SAF} = 0.80 \cdot CI_{Jet\ A-1} + 0.15 \cdot CI_{bio-SAF} + 0.05 \cdot CI_{e-SAF}$$
$$76.125 gCO_2/MJ = 0.80 \cdot 89 gCO_2/MJ + 0.15 \cdot 27.3 gCO_2/MJ + 0.05 \cdot 16.6 gCO_2/MJ \quad (17)$$

$$p_{80/20\ C/SAF} = 0.80 \cdot p_{Jet\ A-1} + 0.15 \cdot p_{bio-SAF} + 0.05 \cdot p_{e-SAF}$$
$$p^{min}_{80/20\ C/SAF} = €0.60/\mathrm{L} = 0.80 \cdot €0.50/\mathrm{L} + 0.15 \cdot €1.00/\mathrm{L} + 0.05 \cdot €1.00/\mathrm{L} \quad (18)$$
$$p^{max}_{80/20\ C/SAF} = €0.69/\mathrm{L} = 0.80 \cdot €0.50/\mathrm{L} + 0.15 \cdot €1.25/\mathrm{L} + 0.05 \cdot €2.00/\mathrm{L}$$

The purpose of holding the price of Jet A-1 constant, despite expectations of the fuel price to grow with time [34], is to isolate the changes in the sustainability performance to the SAF blending levels between the present versus 2035 operational scenarios given both fleets comprise of 100% conv. MAX aircraft. Similarly, the inputs for the passenger traffic, the airport network and the number of aircraft within the fleet were kept constant throughout all studies such that differences between operational scenarios are due solely to variations in the energy carriers, their reconfigured aircraft technologies and decision weights associated with those alternative energy carriers (fuel price, emissions' penalisation, WtW CI, etc.). Therefore, the differences in the resulting sustainability performances may only be attributed to the interaction of these changes in pricing and WtW CI values due to SAF or alternative energy carrier inclusions as well as the increase in $CO_2$ emissions' penalisation ansd highlight the opportunity for decarbonisation posed by these changes to the fuelling practices of the sector.

## 2.3 Alternative Energy Carrier Scenario Definitions

Three alternative energy carrier fuelled aircraft are studied in this work, namely being fuelled with LNG, RNG and $LH_2$. The LNG and RNG fuels are simulated by the previously discussed NG MAX variant and the $LH_2$ MAX variant captures the introduction of $LH_2$ as an energy carrier to the model. These scenarios are compared to the 2035 baseline fleet of conv. MAX aircraft fuelled with the blend of 80% conventional Jet A-1, 15% bio-SAF and 5% e-SAF, the 80/20 C/SAF fuel blend. Each of the three alternative energy carrier aircraft comparative studies are run under a best- and worst-case cost scenario. Furthermore, the different scenarios are split into three fleet compositional sub-cases to highlight the impact of alternative energy carrier availability. These compositional sub-cases are:

1) Two thirds of the fleet being conv. MAX
2) Half of the fleet being conv. MAX
3) One third of the fleet being conv. MAX

In each sub-case per scenario above, the balance of the fleet is the alternative energy carrier MAX variant. Hence, with three alternative energy carrier strands, each with two cost scenarios and a further three fleet compositional sub-cases, 18 distinct alternative energy carrier scenarios are defined

and studied using the previously discussed framework for the purpose of comparing the decarbonisation potential of the alternative energy carriers in a 2035 context. The difference in setup information of the 18 comparative scenarios is denoted in Table 4 with the changes to key parameters such as fleet composition, alternative fuel price, WtW CI and case number. As was the case for the 2035 baseline versus present-day scenarios, the EU ETS rate for $CO_2$ penalisation for all comparative scenarios was set at €200/1000kg of $CO_2$ [40]. Lastly, the alternative energy carrier MAX variants must complete asynchronous turnarounds which is different to the conv. MAX's synchronous turnaround logistics. A synchronous turnaround is the simultaneous actions of passenger on/off-boarding and aircraft refuelling, as described by Figure 15. This is due to the expectation that cryogenic fuels will impact the refuelling practices at airports necessitating the separation of passenger on/off-boarding and the refuelling [41]. As such, two refuel rates, a higher and lower rate of fuel transfer (derived from [41]), are used in the min. and max. cost (best- and worst-case) scenarios to investigate if increased complexity at turnaround for alternative energy carriers impacts the operability of the aircraft types. The min. cost scenario is an optimistic fuel pricing, hence the higher refuel rate (resulting in expectedly shorter turnarounds and crew costs) is assigned to the min. scenarios whereas the lower refuel rate is assigned to the max. cost (worst-case) scenarios. From Figure 15, the turnaround times of the alternative MAX variants are a function of the variable refuelling times, which in turn, are a function of the refuel rates.

Table 4: Comparative study definitions & details

| Strand | LNG Scenarios | | | | | | RNG Scenarios | | | | | | $LH_2$ Scenarios | | | | | |
|---|---|---|---|---|---|---|---|---|---|---|---|---|---|---|---|---|---|---|
| Min./Max. | Min. | | | Max. | | | Min. | | | Max. | | | Min. | | | Max. | | |
| Case No. | 1 | 2 | 3 | 4 | 5 | 6 | 7 | 8 | 9 | 10 | 11 | 12 | 13 | 14 | 15 | 16 | 17 | 18 |
| No. Conv. MAX | 20 | 15 | 10 | 20 | 15 | 10 | 20 | 15 | 10 | 20 | 15 | 10 | 20 | 15 | 10 | 20 | 15 | 10 |
| No. Alt. MAX | 10 | 15 | 20 | 10 | 15 | 20 | 10 | 15 | 20 | 10 | 15 | 20 | 10 | 15 | 20 | 10 | 15 | 20 |
| Refuel Rate | 7661L/min | | | 1216L/min | | | 7661L/min | | | 1216L/min | | | 7661L/min | | | 1216L/min | | |
| Alt. Fuel Cost (Equiv. in €/GJ) | $6/MMBTU [42] | | | $17/MMBTU [42] | | | $15/GJ [43] | | | $22/GJ [43] | | | €0.30/kg [44] | | | €12.38/kg [44] | | |
| | €5.23/GJ | | | €11.34/GJ | | | €13.80/GJ | | | €20.24/GJ | | | €2.48/GJ | | | €102.31/GJ | | |
| Alt. WtW CI | 76g$CO_2$/MJ [45, 46] | | | | | | 19.9g$CO_2$/MJ [46, 47, 48] | | | | | | 34.3g$CO_2$/MJ [49] | | | | | |

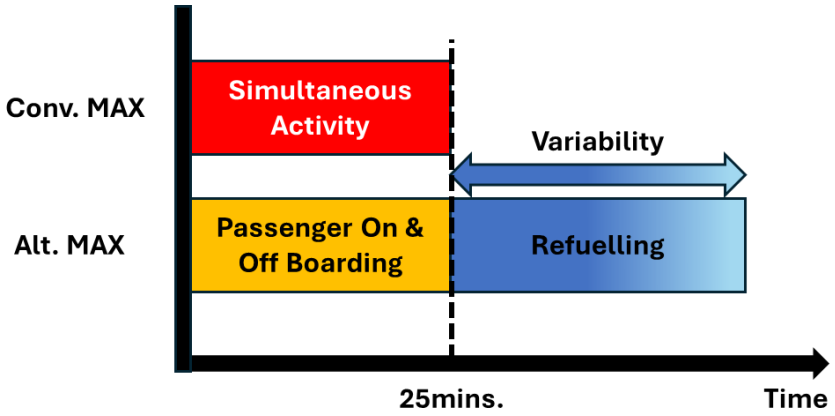



Figure 15: Synchronous (conv. MAX) versus asynchronous (alt. MAX) turnaround practices

## 3. Results & Discussion

The results of the comparative studies are delineated into two main comparative sets. Firstly, the 2035 baseline versus the present day, 100% fossil Jet A-1 fuelled, all conv. MAX fleet. And secondly, the 2035 baseline versus the three alternative energy carrier aircraft.

## 3.1 Present (2026) versus 2035 Baseline

Figure 16 compares the 2035 baseline worst- and best-case cost scenarios to the present, validation scenario along the total passenger capture and revenue breakdown. The results are normalised to the validation scenario in this comparative set to demonstrate the impact to these metrics from the limited change of fuel blending WtW CI reduction, fuel price increase and EU ETS increase.

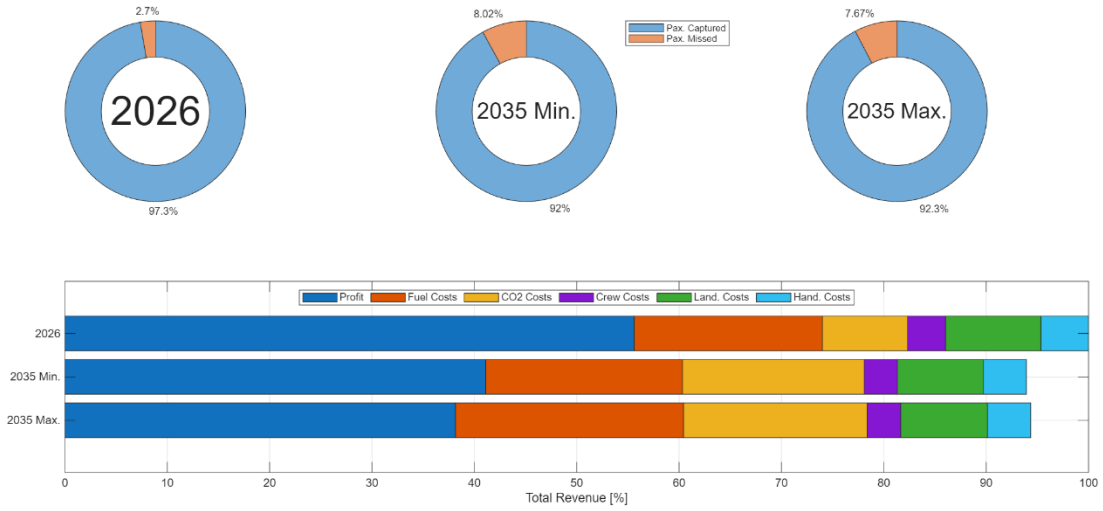



Figure 16: Passenger and revenue breakdown of present versus 2035 baseline scenarios

The total passenger capture is reducing between the 2026 and both 2035 cases due to the increase in operating costs arising from using higher priced 80/20 C/SAF fuel. The bar chart plot in Figure 16 is the revenue breakdown per scenario with the present-day scenario being the normalised basis for comparison. This plot can be understood to indicate the performance of each scenario with the relative size of the darker blue component ("profit") conveying the overall impact on the holistic sustainability metric between cases. The total length of each scenario's bar is the revenue captured per scenario. The red, yellow, purple, green and light blue components are the costs, hence the total length (revenue) less the cost components' lengths give the length of the profit (darker blue) components per scenario, and thus the objective score per scenario. To achieve higher profit, and therefore a stronger holistic sustainability score, a scenario needs to do one of three things during its scheduling of operations: 1) minimise costs and maintain revenue by flying the same number of passengers on less expensive, more efficient aircraft for example, 2) maximise revenue and maintain costs by flying more passengers on more economical aircraft for example or 3) simultaneously maximise revenue while minimising costs.

The total revenues captured in the 2035 min. and max. cases are very similar which is expected given a very similar passenger capture rate (92% and 92.3%, respectively, as read from the donut charts in Figure 16), however both have a modest reduction (~5%) in revenue capture relative to the present-day scenario due to the increase in fuel price and EU ETS penalties on $CO_2$ emissions. The increase in fuel and $CO_2$ costs between the present and 2035 scenarios reduces the revenue capture and profitability which can be seen by the relative length of the red and yellow bars between scenarios. The yellow bar is its narrowest in the present-day scenario, however with the EU ETS near tripling from €70 to €200/1000kg of $CO_2$, the 2035 min. and max. cases suffer a much more significant penalisation for producing emissions with the yellow bar growing considerably. It must also be noted that the widths of the yellow components are near identical for the 2035 scenarios indicating a similar amount of $CO_2$ emissions were produced in both scenarios, which is to be expected given the like-for-like passenger capture values of the scenarios. Similarly, the red bar lengths increase from the present-day scenario to the 2035 min. and max. scenarios with the widest, most costly fuel scenario being the 2035 max. scenario, as expected.

The pairing of higher fuel costs and emissions' penalisation hampers the ability of the 2035 fleet to capture the same amount of revenue in both the worst- and best-case pricing scenarios relative to the present-day scenario. Furthermore, the increase in fuel pricing and emissions' penalisation significantly reduces the profitability, and indeed the holistic sustainability score, of the 2035 scenarios

by contributing more heavily to the costs reducing an already diminished revenue level. Hence, despite the emissions' reduction potential of the 80/20 C/SAF fuel blend for the 2035 scenarios, the fuel pricing and EU ETS levels out-weigh the benefits to be offered through SAF blending alone.

## 3.2 2035 Baseline versus 2035 Alternative Energy Carriers

The second of the comparative sets is the alternative energy carrier scenarios versus the 2035 baseline scenarios. The total revenue captures per scenario and then changes in revenue, profit, fuel and $CO_2$ costs with respect to the baseline 2035 scenarios along the min. and max. cost strands are shown in Figure 17 and Figure 18, respectively.

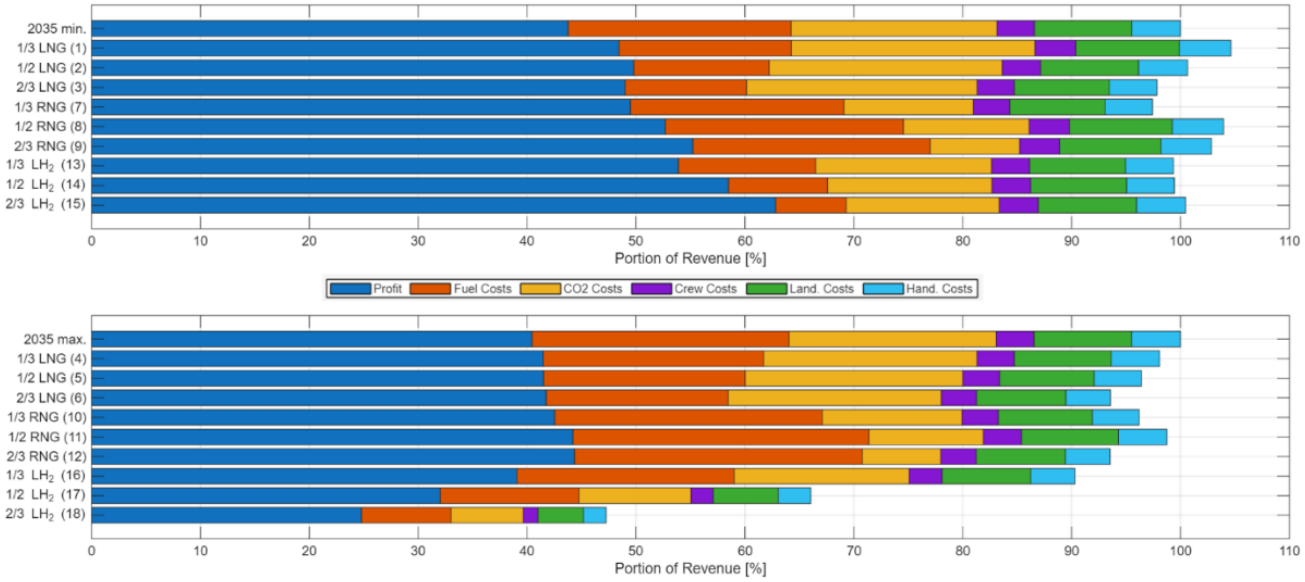



Figure 17: Total revenue capture per scenario for best- (top) & worst-case (bottom) fuel costs

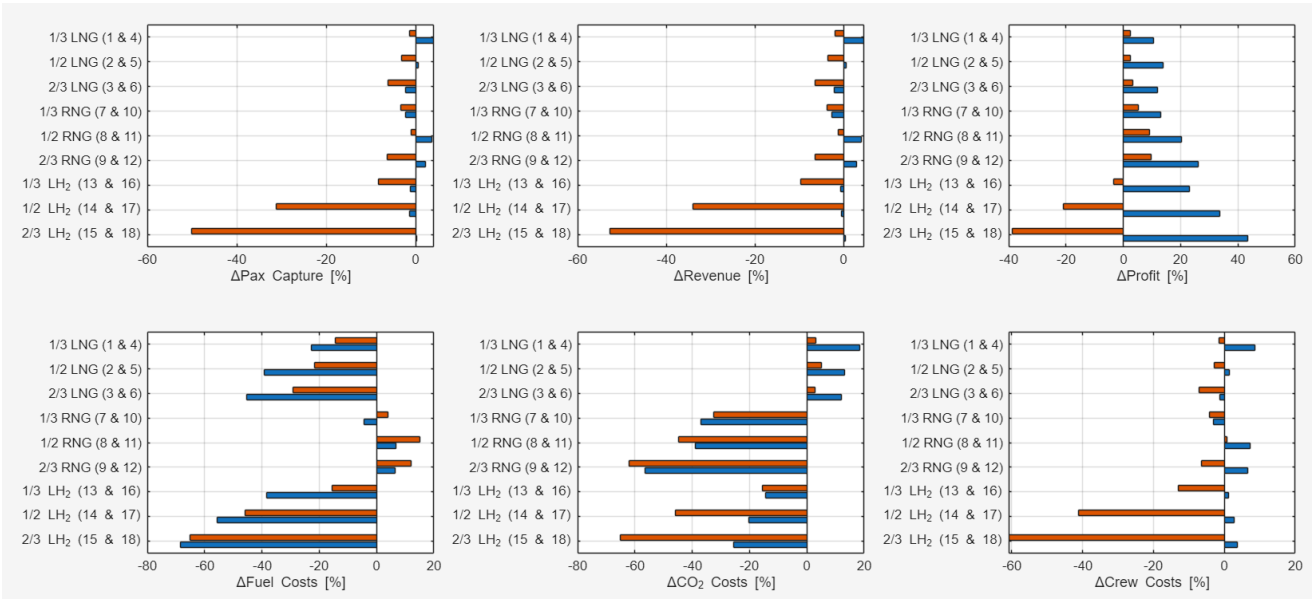



Figure 18: Min. & max. changes w.r.t the 2035 baseline scenarios

Firstly, the row labels per plot in both above Figures denote the fleet composition, alternative energy carrier variant MAX and relevant case numbers that can be cross-referenced with Table 4. For example, the first row "1/3 LNG (1 & 4)" in Figure 18 indicates that the results in this row of the bar chart belong to cases 1 (min.) and 4 (max.), which both use a 1/3 third fleet composition of NG MAX aircraft fuelled by LNG. The difference between the red (max. cost, worst-case scenario) and blue (vice versa) bar lengths per row convey the lower and upper bounds of change in each plot for the metrics of passenger capture (top-left), revenue capture (top-middle), profit (top-right), fuel costs (bottom-left), $CO_2$ costs (bottom-middle) and crew costs (bottom-right). The changes in these metrics

presented in Figure 18 are validated by the total bar and relevant component lengths in Figure 17. Like it was shown for the results of the 2035 baseline scenarios versus the present-day scenario in Figure 16, the revenue capture and passenger capture are directly proportional. This directly proportional relationship again exists for the alternative energy carrier scenarios in Figure 18. There is a non-linear trend in revenue and passenger capture across the scenarios with respect to fleet composition where the increase in alternative energy carrier aircraft doesn't consistently increase or decrease the revenue and passenger capture across the three MAX variants. For example, the LNG scenarios' (first three rows) changes in revenue and passenger capture decreases pseudo-linearly with an increase in LNG MAX availability, however this trend does not reappear for the RNG scenarios (second three rows). Interestingly, the $LH_2$ scenarios (last three rows) have a very broad impact on revenue and passenger capture. The min. cost scenarios have very little change to the capture rate relative to the 2035 baseline which indicates the strong operability of the $LH_2$ aircraft under these costs and scenario parameters. However, the max. cost $LH_2$ scenarios' results all drastically reduce the revenue and passenger capture (with over 50% revenue loss in case 18, red bar of last row). This indicates the in-operability of the same asset under the worst-case fuel cost scenarios.

While the revenue captures, and indeed passenger captures, are one component of the holistic sustainability performance where higher revenue maximises this metric, the changes in fuel and $CO_2$ costs reduce these revenues and ultimately determine the profit scores per scenario. As discussed previously, there is very little difference in the revenue capture of the $LH_2$ min. cost scenarios (blue bars of last three rows in Figure 18), but the profitability scores of these same scenarios are some of the highest achieved. This superior profitability performance for the min. cost $LH_2$ scenarios are not repeated in the max. cost scenarios where the lowest profitability scores are achieved. This is due to the pricing of the fuel in each of these max. cost scenarios, whereas the very favourable price of $LH_2$ in cases 13, 14 and 15 considerably reduce fuel costs while maintaining high revenue capture therefore boosting profits tremendously for the min. cost scenarios. The LNG and RNG scenarios do not demonstrate the same broadness in their upper and lower bounding of operability and profitability scores between the min. and max. cost scenarios. Both the LNG and RNG scenarios all consistently have improved profitability compared to the 2035 baseline scenarios in both the worst- and best-case cost strands. However, the relatively higher $CO_2$ costs for the LNG (due to the higher WtW CI values of LNG compared to RNG) result in the RNG being the most consistently, holistically sustainable alternative energy carrier in both min. and max. scenarios.

Earlier it was stated that the decision weight values against crew costs were not varied across the different scenarios, however variations in the accumulated crew costs can be seen in Figure 18. The reason these costs are varying despite no change to their weights is due to the number of flights and the change in turnaround logistics due to asynchronous turnarounds for the alternative energy carriers as discussed in Section 2.3 and Figure 15. The variable refuel rate (as seen in Table 4) values change between scenarios relative to the conv. MAX aircraft and thus change the turnaround times after flights. This increase to the turnaround time due to variable refuel rates can be seen with the trend of crew costs growing with the higher availability of the alternative energy carrier variant MAX aircraft within the fleet. However, the variable refuel rates and ultimate impact on the crew costs had less influential, more secondary impacts on the profitability relative to the more dominating fuel costs and $CO_2$ costs, as seen by the relative bar widths of the constituent parts in Figure 17. The crew costs' trends across scenarios mirrors that of the passenger and revenue captures' trends in Figure 18, indicating a reactionary-behaviour by the crew costs to the number of flights (more flights gives more revenue and passenger capture, with the inverse leading to lower profit) rather than guiding the framework's optimisation of the schedule through selection of missions based on their turnaround times. Conversely, the fuel and $CO_2$ costs strongly influence the framework's optimisation due to their more direct impact on the profit per mission. As such, the balance of power within the objective function (and ultimately, the optimisation of the schedule) can be understood to be primarily driven by maximising revenue through passenger capture while simultaneously minimising the fuel and $CO_2$ costs (in-flight performances) first, then being considerate of the crew costs second due to their lesser influence. These data result in the ranking of the alternative energy carrier options as RNG being the most beneficial, LNG being a second-best, consistently beneficial option while $LH_2$ was only viable in the min. cost scenarios and completely inoperable in the max. cost scenarios.

Figure 19 and Figure 20 show the PSEC performances of the various scenarios but extended to a WtW scale to account for the energy required to generate the fuels (the Well-to-Tank, WtT side). The WtW PSEC metric is an extension of the previously shown Tank-to-Wake (TtW) scale, conventional PSEC values from the aircraft performance sub-model discussion in Section 2.1.1. The WtW PSEC metric, defined in Equation (20), is the ratio of the total WtW energy demand (generation and operation) to complete the mission and the revenue passenger energy from said mission. The WtT side of the total energy demand, the generation energy ($E_{gen}$), is calculated using the WtT production efficiency ($\eta_p$) of each fuel pathway as defined by Equation (19). The production efficiency denotes how much input energy (generation energy) to the pathway is required to generate an amount of useable fuel ($E_{fuel}$). The TtW side of the total energy, the consumption energy ($E_{cons}$) is the previously discussed fuel consumption as determined via the aircraft performance sub-model. The production efficiencies used in this analysis are denoted in Table 5 for each of the fuels in addition to these resulting generation energies required to produce 1MJ of consumable fuel for each of the fuel types.

$$\eta_p = \frac{E_{fuel}}{E_{gen}} \rightarrow E_{gen} = \frac{E_{fuel}}{\eta_p} \tag{19}$$

$$PSEC_{WtW} = \frac{E_{gen} + E_{cons}}{E_{RPK}} = \frac{E_{WtT} + E_{TtW}}{E_{RPK}} = \frac{E_{WtW}}{E_{RPK}} \tag{20}$$

Table 5: Fuel pathway production efficiencies

| *Fuel Type* | *Prod. Efficiency (%)* | *Gen. Energy required per 1MJ of fuel (MJ)* |
|---|---|---|
| Jet A-1 | 91.0 [50] | 1.0989 |
| Bio-SAF | 43.6 [15] | - |
| e-SAF | 30.3 [15] | - |
| 80/20 C/SAF | - | 1.3882 |
| LNG | 90.1 [51] | 1.1099 |
| RNG | 42.7 [51] | 2.3407 |
| $LH_2$ | 55.7 [52] | 1.7953 |

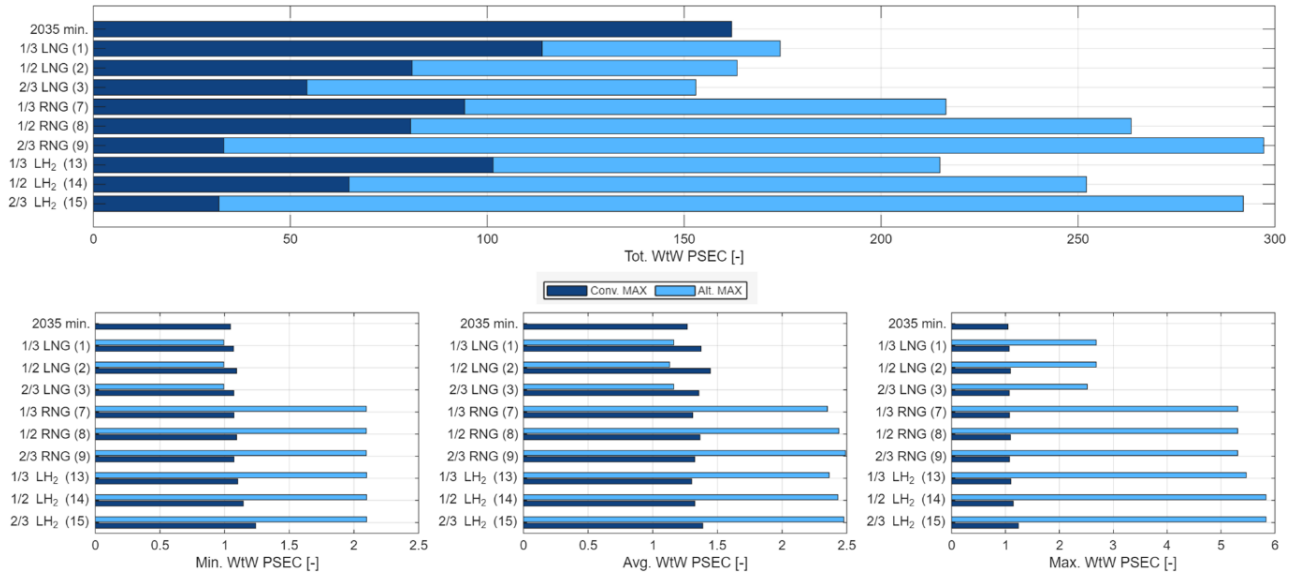



Figure 19: Min. cost scenarios WtW PSEC performances

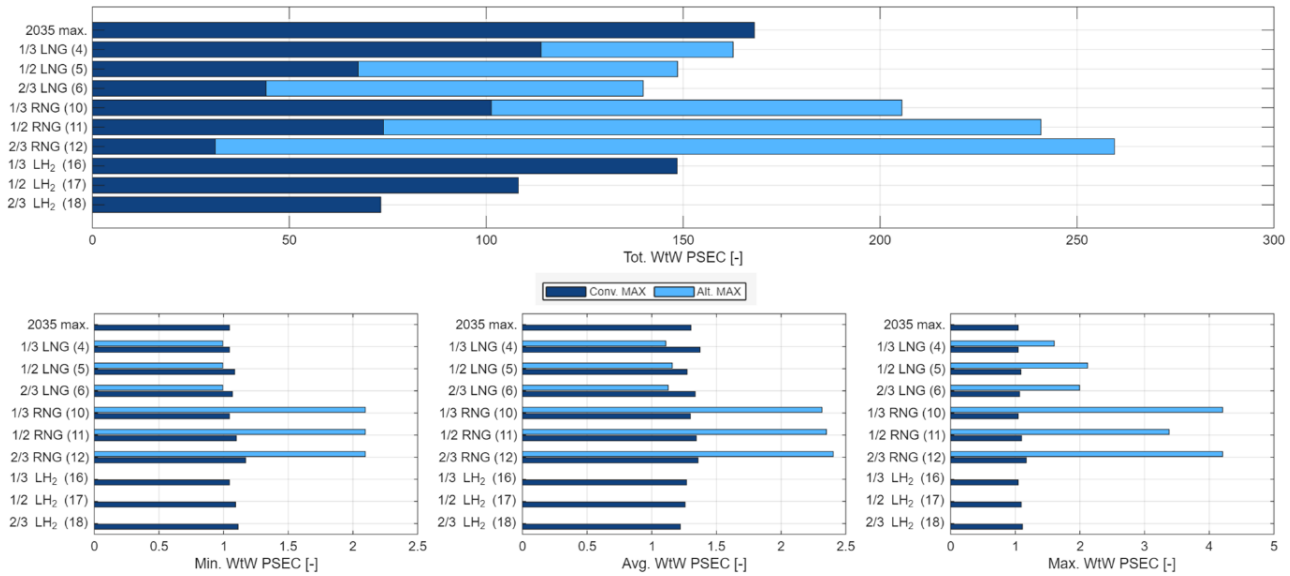



Figure 20: Max. cost scenarios WtW PSEC performances

Figure 19 and Figure 20 show the breakdown of the WtW PSEC performances for the min. and max. cost scenarios, respectively. The dark blue bar represents the contributions from the conv. MAX aircraft within the fleet while the light blue bars represent the contributions from the alternative energy carrier MAX aircraft (denoted as “Alt. MAX” in the legend) per scenario. Firstly, the trends discussed previously in relation to revenue capture and operability of the different aircraft types appear again in the WtW PSEC plots. The $LH_2$ aircraft is unusable in the max. cost scenarios as seen in Figure 20, where there are no $LH_2$ MAX aircraft contributions (light blue bar) to the total, minimum, average or maximum WtW PSEC sub-plots. The alternative energy carrier MAX variants all suffer from increased in-flight (TtW) energy consumption. The 80/20 C/SAF production efficiency is better than the RNG and $LH_2$ fuels but is higher than LNG. These relative differences between in-flight performance and production efficiency impact the WtW PSEC performance by making RNG and $LH_2$ more demanding than 80/20 C/SAF. However, the LNG is less demanding from an energy perspective than the 2035 baseline fuel. This manifests in the min. cost scenarios of Figure 19 where the various WtW PSEC values are always larger than the 2035 baseline for the RNG and $LH_2$ scenarios. Similarly, the size of the light blue bars grows with an increase in the number of RNG or $LH_2$ aircraft in the fleet indicating the operability of the different aircraft types and higher contribution to these larger WtW PSEC values. This trend of generally higher WtW PSEC values and strictly increasing with availability of alternative energy carrier aircraft does not hold for the LNG scenarios in Figure 19. In fact, the WtW PSEC trend for the LNG scenarios are inversed, the LNG scenarios always have a reduced WtW PSEC performance relative to the 2035 baseline and continue to decrease it further with higher LNG aircraft availability. The max. cost scenarios of Figure 20 convey similar trends for the LNG and RNG scenarios confirming the energy demand trends previously discussed. The $LH_2$ MAX was inoperable in the max. cost scenario due to the disparity of fuel pricing, potential emissions’ reduction through WtW CI, emissions’ penalisation and the severe in-flight energy penalty relative to the conv. MAX.

The higher energy penalties associated with using the alternative MAX variants (as shown in Figure 9 and Figure 10 from Section 2.1.1), necessitate higher energy consumption to complete the same mission for the alternative energy carriers. Factoring in the generation side of the fuels better characterises the viability of the alternative energy carrier pathways. Earlier in the results, it was seen that the RNG scenarios achieved consistently superior holistic sustainability performances versus the LNG, $LH_2$ (max. cost scenarios) and 2035 baseline scenarios. However, when reviewing the energy demand and productive use of said energy for each scenario from a WtW perspective in Figure 19 and Figure 20, it is clear that LNG achieves the most energy-effective pathway of these scenarios. The holistic sustainability scores of the RNG scenarios outperformed the LNG ones due to more effective combinations of emissions reduction and fuel pricing, however the RNG scenarios have the highest WtW PSEC values of all scenarios indicating the true cost of adopting that alternative energy carrier pathway. Furthermore, this calls on the need for out-of-sector enablers related to the production of RNG and other lower-carbon fuels to materialise, improve and offer further

decarbonisation potential. This more complete view of the decarbonisation potential via the holistic sustainability score in combination with an understanding of WtW PSEC requirements to achieve this score, highlights the need to revisit the ranking of the alternative energy carrier scenarios. The RNG scenarios achieve the best sustainability scores but demand the most energy to achieve these. The LNG scenarios achieve comparatively strong sustainability scores which consistently beat the 2035 baseline scenarios but are lower than the RNG ones, however the LNG scenarios offer the lowest energy demand in achieving these scores. The $LH_2$ scenarios only offer sustainability score improvements in the min. cost scenarios and demand more energy to achieve these scores therefore limiting its operability and viability as a decarbonisation pathway in its current configuration. Being guided solely by the holistic sustainability metric, the RNG still remains the most attractive alternative energy carrier, but its considerable energy demand highlights the need to include the WtW PSEC performance of an alternative energy carrier in the design and re-configuration component of this framework to better leverage the sustainability benefits offered from said energy carrier concepts.

## 4. Conclusions

The simulation of the 2035 baseline scenarios versus the present-day scenario demonstrated that the modus operandi of the sector will change between now and 2035 with mandated SAF blending. This comparative set kept the technology level as well as the operations the same through the conv. MAX fleet and the use of an identical airport network and passenger traffic input, respectively. The energy carrier, market-based measures and policy levels changed between the present and 2035 scenarios. The energy carrier shifted from 100% fossil Jet A-1 to a SAF blend of 80% fossil Jet A-1, 15% bio-SAF and 5% e-SAF, which in turn changed the market-based measures of fuel pricing. Lastly, the EU ETS penalisation level for $CO_2$ emissions increased from €70 to €200/1000kg of $CO_2$. These changes in the decarbonisation themes led to a decrease in both the passenger capture and final holistic sustainability score which highlighted the gap in the design space for alternative energy carriers to not only address the decarbonisation challenge but offer viably economic and environmental options for technology and operations.

The alternative energy carriers used were fossil LNG, a lower carbon-intensity RNG candidate, and $LH_2$. These fuels necessitated the re-configuration of the conv. MAX aircraft to the NG MAX (for the LNG and RNG fuels) and $LH_2$ MAX which were a dry-wing, fuselage-based cryogenic fuel tank variant of the MAX capable of delivering the same design mission, reserve mission, and other pertinent TLARs. The change in energy carrier of the conv. MAX significantly altered its in-flight performance post re-configuration with both the NG MAX and $LH_2$ MAX variants having considerable increases in their TtW PSEC characteristics across the full operating range of the aircraft, with the $LH_2$ variant suffering the most. The purpose of using the alternative energy carriers was to leverage the benefits from their WtW CI compared to fossil Jet A-1, however it isn't enough to assume a fuel's lower WtW CI will have tangible impacts on decarbonisation potential. The scheduling scenarios comparing different permutations of fuel pricing, fleet composition and aircraft type demonstrated that the problem of addressing the decarbonisation potential through alternative energy carriers is highly multi-faceted and complex. The full potential of the lower WtW CIs weren't always possible to be leveraged due a combination of interactions with higher fuel pricing, higher in-flight energy demand and sterner emissions' penalisation. As such, the alternative energy carrier which had the most compatible combination of WtW CI, in-flight energy consumption and fuel pricing and hence, achieved the most improved sustainable performance relative to the baseline was RNG. Conversely, the $LH_2$ was only operable in the min. cost scenarios where it boasted strong holistic sustainability scores, however with it being completely unviable in the max. cost scenarios, the lack of an upper bound rendered its consideration as a decarbonisation concept in its current configuration moot.

This work has considered a variety of alternative energy carrier options for the decarbonisation of the aviation sector with a bounded prediction for lower and upper cost scenarios to clarify the potential offered by the concepts considered. The alternative energy carriers required the reconfiguration of the technologies used which have been proven to be sub-optimal aircraft designs after simulating their application through the scheduling of operations. The scheduling component of the framework brought into consideration the true impact and viability of the decarbonisation concepts through an objective analysis of its holistic sustainability. The interactions of reduced WtW CI, fuel pricing, emissions' penalisation and mission-specific costs led the scheduler to find optimal schedules that used the different aircraft variants in a way that maximised the holistic sustainability scores per

scenario. Ultimately, the RNG offered the most sustainability potential with further possible advantages to be gained from continued re-design and optimisation of the NG airframe to become more operationally efficient via reduced energy consumption, utilisation of improved technologies and tailoring of the TLARs to the specific energy carrier. This of course would further improve the LNG scenarios (given both energy carriers used the NG MAX airframe) lending further credence to the idea of using natural gas as an alternative energy carrier within aviation.

Through the definition of a novel WtW PSEC metric for the purpose of better evaluating the potential of alternative energy carriers, this work was able to determine that the LNG scenarios had the lowest WtW PSEC requirements paired with comparatively strong sustainability scores, whereas the RNG scenarios had the largest WtW PSEC values paired with the best sustainability scores. The difference between LNG and RNG is the WtT generation component of its pathway. Hence, natural gas' inclusion as an alternative energy carrier for aviation has been reinforced with its "greenest" variant (RNG) achieving the best holistic sustainability scores of all scenarios, while its most energy-efficient variant (LNG) still achieves favourable sustainability scores. Unfortunately, confidence in the application of $LH_2$ was not gained through this work. The $LH_2$ MAX's in-flight energy performance decrement was too severe. This was exacerbated when paired with a very undesirable upper bound for $LH_2$ fuel pricing, meaning its potential advantages through a lower WtW CI were unachievable in the current configuration. The $LH_2$ MAX requires a significant amount of re-design and optimisation from an in-flight energy consumption perspective to even be in consideration for application. In conclusion, the framework was capable of modelling all the necessary functionality and provide comparative, objective evaluations for the holistic sustainability performances of alternative energy carrier scenarios. The framework demonstrated the holistic sustainability gains available from LNG and RNG as well as the limited potential of $LH_2$ in its current configuration. Thus, it provided recommendations of how to leverage and address the advantages and drawbacks through more optimised pairings of aircraft in-flight performances, fuel prices and $CO_2$ penalisation.

## 5. Contact Author Email Address

mailto: Mr. Naoise Barry at nabarry@tcd.ie

## 6. Copyright Statement

The authors confirm that they, and/or their company or organisation, hold copyright on all of the original material included in this paper. The authors also confirm that they have obtained permission, from the copyright holder of any third party material included in this paper, to publish it as part of their paper. The authors confirm that they give permission, or have obtained permission from the copyright holder of this paper, for the publication and distribution of this paper as part of the ICAS proceedings or as individual off-prints from the proceedings.

## Acknowledgements

The authors would like to thank Ryanair for their technical support of this study through the use their data.

## References

[1] International Civil Aviation Organisation - ICAO, "Wings of Prosperity - Economic Growth Through Air Transport," 2024. [Online]. Available: https://www.icao.int/sites/default/files/sustainability/Documents/Wings-of-Prosperity-August-2024-2.pdf. [Accessed May 2026].

[2] Aviation Benefits Beyond Borders, "European Union - Aviation's Economic Impact," 2023. [Online]. Available: https://aviationbenefits.org/media/mjokvnkd/abbb2024_eu27.pdf. [Accessed May 2026].

[3] Air Transport Action Group - ATAG, "Aviation and Climate Change - Waypoint 250 Fact Sheet #2," December 2024. [Online]. Available: https://atag.org/media/gw5cgzzh/fact-sheet_2_aviation-and-climate-change.pdf. [Accessed May 2026].

[4] International Air Transport Association - IATA, "IATA Long-Term Air Transport Passenger Demand Projections," February 2026. [Online]. Available: https://www.iata.org/en/iata-

repository/publications/economic-reports/iata-long-term-air-transport-passenger-demand-projections/. [Accessed May 2026].

[5] International Air Transport Association - IATA, “Aviation Benefits Beyond Borders - Waypoint 2050,” [Online]. Available: https://aviationbenefits.org/other-environmental-challenges/climate-action/waypoint-2050/. [Accessed May 2026].

[6] United Nations - UN, “Climate Change - The Paris Agreement,” 2015. [Online]. Available: https://unfccc.int/process-and-meetings/the-paris-agreement. [Accessed May 2026].

[7] The European Union - EU, “Energy, Climate Change, Environment - Reducing emissions from aviation,” [Online]. Available: https://climate.ec.europa.eu/eu-action/transport-decarbonisation/reducing-emissions-aviation_en. [Accessed May 2026].

[8] International Air Transport Association - IATA, “Sustainability - Fly Net Zero - Net Zero Roadmaps,” [Online]. Available: https://www.iata.org/en/programs/sustainability/flynetzero/roadmaps/. [Accessed May 2026].

[9] International Air Transport Association - IATA, “Net zero carbon 2050 resolution - Fact Sheet,” [Online]. Available: https://www.iata.org/en/iata-repository/pressroom/fact-sheets/fact-sheet-iata-net-zero-resolution/. [Accessed May 2026].

[10] International Civil Aviation Organisation - ICAO, “Long Term Global Aspirational Goal (LTAG) for international aviation,” 2022. [Online]. Available: https://www.icao.int/environmental-protection/LTAG. [Accessed May 2026].

[11] International Civil Aviation Organisation - ICAO, “Uniting Aviation - ICAO's Stategic Goals explained: Achieving net-zero carbon emissions by 2050,” Dec 2025. [Online]. Available: https://unitingaviation.com/news/environment/icaos-strategic-goals-explained-achieving-net-zero-carbon-emissions-by-2050/. [Accessed May 2026].

[12] Navarrete, A: The International Council on Clean Transportation - ICCT, “Understanding the greenhouse gas emissions of different SAF pathways,” Oct 2025. [Online]. Available: https://theicct.org/understanding-the-ghg-emissions-of-different-saf-pathways-sept25/. [Accessed May 2026].

[13] European Union Aviation Safety Agency - EASA, “Environment - What are Sustainable Aviation Fuels?,” [Online]. Available: https://www.easa.europa.eu/en/domains/environment/eaer/sustainable-aviation-fuels/what-are-sustainable-aviation-fuels#two-options-for-100-saf-drop-in-and-non-drop-in. [Accessed May 2026].

[14] F. Nyholm, S. Toppinen and H. Saxén, “Sustainable power-to-liquids aviation fuels: Modelling and comparison of two Fischer-Tropsch upgrading process concepts,” Energy Converion and Management, October 2025. [Online]. Available: https://doi.org/10.1016/j.enconman.2025.120153.

[15] R. G. Grim, D. Ravikumar, E. C. D. Tan, Z. Huang, J. R. Ferrell III, M. Resch, Z. Li, C. Mevawala, S. D. Philips, L. Snowden-Swan, L. Tao and J. A. Schaidle, “Electrifying the production of sustainable aviation fuel: the risks, economics, and environmental benefits of emerging pathways including CO2,” Energy & Environmental Sciences, November 2022. [Online]. Available: https://doi.org/10.1039/D2EE02439J.

[16] NASA, “Electrified aircraft propulsion: N3-X,” 2022. [Online]. Available: https://www.nasa.gov/eap-aircraft-concepts/n3-x/. [Accessed June 2026].

[17] Aviation Benefits Beyond Borders, “Producing sustainable aviation fuel,” [Online]. Available: https://aviationbenefits.org/other-environmental-challenges/climate-action/sustainable-aviation-fuel/producing-sustainable-aviation-fuel/. [Accessed May 2026].

[18] The European Union - UN, “Mobility and Transport - ReFuelEU Aviation,” [Online]. Available: https://transport.ec.europa.eu/transport-modes/air/environment/refueleu-aviation_en. [Accessed May 2026].

[19] M. Bazargan, “Airline Operations and Scheduling,” 2010 (2nd Edition). [Online]. Available: https://doi.org/10.4324/9781315566474.

[20] S. Roy, W. A. Crossley, K. T. Moore, J. S. Gray and J. R. R. A. Martins, “Monolithic Approach for Next-Generation Aircraft Design Considering Airline Operations and Economics,” AIAA ARC, 2019. [Online]. Available: https://doi.org/10.2514/1.C035312.

[21] M. Hoogreef, N. Zuijderwijk, E. Scheers, P. Proesmans and B. F. Santos, “Coupled Hybrid & Electric Aircraft Design and Strategic Airline Planning,” AIAA ARC, 2023. [Online]. Available: https://doi.org/10.2514/6.2023-3869.

[22] K. Moolchandani, P. Govindaraju, S. Roy, W. A. Crossley and D. A. DeLaurentis, “Assessing Effects of Aircraft and Fuel Technology Advancement on Select Aviation Environmental Impacts,” AIAA ARC, 2016. [Online]. Available: https://doi.org/10.2514/1.C033861.

[23] N. Barry, C. Gallagher, S. Fiztgerald and C. Stuart, “CHARACTERISING THE ROLE OF FLEET RENEWAL ON THE PATHWAY TO 2050: A EUROPEAN AIRLINE CASE STUDY,” ICAS Congress 2024, 2024. [Online]. Available: https://www.icas.org/icas_archive/icas2024/data/papers/icas2024_0126_paper.pdf.

[24] N. Barry, C. Gallagher and C. Stuart, “Optimising for Sustainability as an Objective Function Within Airline Fleet Scheduling: An Ireland – EU Mobility Case Study,” AIAA - ARC, 2024. [Online]. Available: https://doi.org/10.2514/6.2024-4166.

[25] G. Gallagher, C. Stuart and S. Spence, “Liquid Hydrogen and Synthetic Sustainable Aviation Fuel: A European Airline Case Study,” Journal of the Global Power & Propulsion Society, Paper, 2025. [Online]. Available: 10.33737/jgpps24/204054.

[26] European Aviation Safety Agency - EASA, “Certification Specifications for Large Aeroplanes CS-25, Amendment 3,” September 2007. [Online]. Available: https://www.easa.europa.eu/sites/default/files/dfu/CS-25_Amdt%203_19.09.07_Consolidated%20version.pdf. [Accessed June 2026].

[27] G. Bower and I. Kroo, “Multi-Objective Aircraft Optimization for Minimum Cost and Emissions over Specific Route Networks,” AIAA - ARC, 2012. [Online]. Available: https://doi.org/10.2514/6.2008-8905.

[28] M. Taflan, H. Smith and J. Loughlan, “Structural sizing and mass estimation of transport aircraft wings with distributed, hydrogen, and electric propulsions,” Royal Aeronautical Society, The Aeronautical Journal, 2024. [Online]. Available: doi:10.1017/aer.2024.117.

[29] National Aeronautics and Space Adminisatration - NASA, “Earth Atmosphere Model,” [Online]. Available: https://www.grc.nasa.gov/www/k-12/airplane/atmosmet.html. [Accessed Jun 2026].

[30] R. C. Boehm, Z. Yang and D. C. Bell, “Lower Heating Value of Jet Fuel From Hydrocarbon Class Concentration Data and Thermo-Chemical Reference Data: An Uncertainty Quantification,” United States. Department of Transportation. Federal Aviation Administration. Center of Excellence for Alternative Jet Fuels and Environment. University of Dayton, 2021. [Online]. Available: https://doi.org/10.1016/j.fuel.2021.122542.

[31] D. Gil-Prieto, G. K. Hristov, D. Neuman, L. Wolfe, F. Giannini, M. Focaracci, A. Kutzmann, M. Neubauer, Z. Hoisington, J. Martinez and N. Quinn, “AACES 2050 Phase I: Technology Identification, Prioitization, and Roadmapping,” AIAA-ARC, June 2026. [Online]. Available: https://doi.org/10.2514/6.2026-4209.

[32] N. Barry and C. Stuart, “Developing Discrete Optimisation Methods for a Holistic Airline Scheduling Algorithm With Sustainability as an Objective Function,” AIAA - ARC, 2026. [Online]. Available: https://doi.org/10.2514/6.2026-0451.

[33] OAG Takeoff, “Data Insights on the World's Major Airlines,” Feb 2025. [Online]. Available: https://www.oag.com/ryanair-performance-stats. [Accessed Jun 2026].

[34] International Air Transport Association - IATA, “Jet Fuel Price Monitor - Sustainability & Economics,” 2026. [Online]. Available: https://www.iata.org/en/publications/economics/fuel-monitor/. [Accessed June 2026].

[35] Ryanair DAC, “Investor Summary 202526 FY26 - Ryanair,” 2026. [Online]. Available: https://investor.ryanair.com/wp-content/uploads/2026/05/FY26-Ryanair-Results.pdf. [Accessed June 2026].

[36] International Air Transport Association - IATA, “IATA Net Zero Progress Report 2024,” 2024. [Online]. Available: https://www.iata.org/contentassets/252e4a52294e4d86928fb5fd8a1ffd5c/netzero-progressreport2024.pdf. [Accessed May 2026].

[37] Boeing, “CASCADE - Documentation: Energy Parameter Bounds,” 2026. [Online]. Available: https://docs.cascade.boeing.com/docs/scenarios/parameterBounds/energy.html#energy-saf-

parameter-bounds. [Accessed June 2026].

[38] International Air Transport Association - IATA, “Global Feedstock Assessment for SAF Production - Outlook to 2050,” September 2025. [Online]. Available: https://www.iata.org/globalassets/iata/publications/sustainability/global-feedstock-assessment-for-saf-production-outlook-to-2050.pdf. [Accessed June 2026].

[39] The Royal Society, “Sustainable synthetic carbon based fuels for transport - Policy Briefing,” September 2019. [Online]. Available: https://royalsociety.org/-/media/policy/projects/synthetic-fuels/synthetic-fuels-briefing.pdf. [Accessed June 2026].

[40] ABN AMRO, “ESG Economist - Scenarios shaping EU ETS prices,” September 2025. [Online]. Available: https://www.abnamro.com/research/en/our-research/esg-economist-scenarios-shaping-eu-ets-prices. [Accessed June 2026].

[41] Aerospace Technology Institute - ATI, “Fly Zero - Hydrogen Infrastructure and Operations, Airports, Airlines and Airspace.,” March 2022. [Online]. Available: https://www.ati.org.uk/wp-content/uploads/2022/03/FZO-CST-POS-0035-Airports-Airlines-Airspace-Operations-and-Hydrogen-Infrastructure.pdf. [Accessed June 2026].

[42] The Oxford Institute for Energy Studies, “The Global Outlook for Gas Demand in a $6 World,” October 2025. [Online]. Available: https://www.oxfordenergy.org/wpcms/wp-content/uploads/2025/10/NG202-The-Global-Outlook-for-Gas-Demand-in-a-6-World.pdf. [Accessed June 2026].

[43] International Energy Agency, “Outlook for Biogas and Biomethane - A global geospatial assessment,” May 2025. [Online]. Available: https://iea.blob.core.windows.net/assets/5b757571-c8d0-464f-baad-bc30ec5ff46e/OutlookforBiogasandBiomethane.pdf. [Accessed June 2026].

[44] F. B. Bozzolo Lueckel, R. F. D. Monaghan and M. Á. Lynch, “Hydrogen supply chain modelling at energy system scale: A review,” Renewable and Suatinable Energy Reviews, March 2025. [Online]. Available: https://doi.org/10.1016/j.rser.2024.115218.

[45] Natural & Bio Gas Vehicle Association (NGVA) Europe, “Greenhouse Gas Intensity of Natural Gas,” Thinkstep, 2017. [Online]. Available: https://gasnam.es/wp-content/uploads/2017/11/NGVA-thinkstep_GHG_Intensity_of_NG_Final_Report_v1.0.pdf.

[46] P. Balcombe, N. P. Brandon and A. D. Hawkes, “Characterising the distribution of methane and carbon dioxide emissions from the natural gas supply chain,” Journal of Cleaner Production, 2018. [Online]. Available: https://doi.org/10.1016/j.jclepro.2017.11.223.

[47] S. Kolb, T. Plankenbuhler, K. Hofmann, J. Bergerson and J. Karl, “Life cycle greenhouse gas emissions of renewable gas technologies: A comparative review,” Renewable and Sustainable Energy Reviews, 2021. [Online]. Available: https://doi.org/10.1016/j.rser.2021.111147.

[48] Sustainable Ships, “Emission Properties for EU ETS, FuelEU and IMO Net-Zero,” Sustainable Ships, 2026. [Online]. Available: https://www.sustainable-ships.org/stories/2025/fuel-emissions-properties. [Accessed Sep 2026].

[49] Boeing, “CASCADE - Documentation: Energy Ambition Levels,” 2026. [Online]. Available: https://docs.cascade.boeing.com/docs/scenarios/ambitionLevels/energy.html#ambition-levels-hydrogen. [Accessed June 2026].

[50] P. Trivedi, H. Olcay, M. D. Staples, M. R. Withers, R. Malina and S. R. H. Barrett, “Energy return on investment for alternative jet fuels,” Applied Energy Vol. 141, March 2015. [Online]. Available: https://doi.org/10.1016/j.apenergy.2014.12.016.

[51] NASA, “AACES Final Report,” 2026. [Online]. Available: https://www.nasa.gov/reference/advanced-aircraft-concepts-for-environmental-sustainability-2050/.

[52] B. C. Tashie-Lewis, “Hydrogen Production, Distribution, Storage and Power Conversion in a Hydrogen Economy - A Technology Review,” Chemical Engineering Journal Advances, August 2021. [Online]. Available: 10.1016/j.ceja.2021.100172.